

Fine Structure and Differentiation of Ascidian Muscle

II. MORPHOMETRICS AND DIFFERENTIATION OF THE CAUDAL MUSCLE CELLS OF *DISTAPLIA OCCIDENTALIS* TADPOLES^{1,2}

MICHAEL J. CAVEY AND RICHARD A. CLONEY

Department of Zoology, University of Washington, Seattle, Washington 98195

ABSTRACT The locomotor function of the caudal muscle cells of ascidian larvae is identical with that of lower vertebrate somatic striated (skeletal) muscle fibers, but other features, including the presence of transverse myomuscular junctions, an active Golgi apparatus, a single nucleus, and partial innervation, are characteristic of vertebrate myocardial cells.

Seven stages in the development of the compound ascidian *Distaplia occidentalis* were selected for an ultrastructural study of caudal myogenesis. A timetable of development and differentiation was obtained from cultures of isolated embryos in vitro.

The myoblasts of the *neurulating embryo* are yolky, undifferentiated cells. They are arranged in two bands between the epidermis and the notochord in the caudal rudiment and are actively engaged in mitosis.

Myoblasts of the *caudate embryo* continue to divide and rearrange themselves into longitudinal rows so that each cell simultaneously adjoins the epidermis and the notochord. The formation of secretory granules by the Golgi apparatus coincides with the onset of proteid-yolk degradation and the accumulation of glycogen in the ground cytoplasm.

Randomly oriented networks of thick and thin myofilaments appear in the peripheral sarcoplasm of the muscle cells of the *comma embryo*. Bridges interconnect the thick and thin myofilaments (actomyosin bridges) and the thick myofilaments (H-bridges), but no banding patterns are evident. The sarcoplasmic reticulum (SR), derived from evaginations of the nuclear envelope, forms intimate associations (peripheral couplings) with the sarcolemma.

Precursory Z-lines are interposed between the networks of myofilaments in the *vesiculate embryo*, and the nascent myofibrils become predominantly oriented parallel to the long axis of the muscle cell.

Muscle cells of the *papillate embryo* contain a single row of cortical myofibrils. Myofibrils, already spanning the length of the cell, grow only in diameter by the apposition of myofilaments. The formation of transverse myomuscular junctions begins at this stage, but the differentiating junctions are frequently oriented obliquely rather than orthogonally to the primary axes of the myofibrils.

With the appearance of H-bands and M-lines, a single perforated sheet of sarcoplasmic reticulum is found centered on the Z-line and embracing the I-band. The sheet of SR establishes peripheral couplings with the sarcolemma.

In the *prehatching tadpole*, a second collar of SR, centered on the M-line and extending laterally to the boundaries with the A-bands, is formed. A single perforated sheet surrounds the myofibril but is discontinuous at the side of the myofibril most distant from the sarcolemma. To produce the intricate architecture of the fully differentiated collar in the *swimming tadpole* (J. Morph., 138: 349, 1972),

¹ This investigation was supported by NIH Developmental Biology Training grant 5-T01-HD00266 to the University of Washington and by NSF Research grant GB 5394.

² Requests for reprints should be directed to Dr. Cloney. The present address of Dr. Cavey is Department of Biological Structure, University of Miami School of Medicine, Miami, Florida 33152.

the free ends of the sheet must elevate from the surface of the myofibril, recurve, and extend peripherally toward the sarcolemma to establish peripheral couplings.

Morphological changes in the nucleus, nucleolus, mitochondria, and Golgi bodies are described, as well as changes in the ground cytoplasmic content of yolk, glycogen, and ribosomes.

The volume of the differentiating cells, calculated from the mean cellular dimensions, and analyses of cellular shape are presented, along with schematic diagrams of cells in each stage of caudal myogenesis. In an attempt to quantify the differences observed ultrastructurally, calculations of the cytoplasmic volume occupied by the major classes of organelles are included.

Comparison is made with published accounts on differentiating vertebrate somatic striated and cardiac muscles.

The location and locomotor function of striated muscle cells from larval ascidians are similar to those of vertebrate somatic striated (skeletal) muscle fibers. In other characteristics, including the mononucleate condition, the presence of transverse myomuscular junctions, numerous close junctions, an active Golgi apparatus, and incomplete innervation, they resemble cardiac muscle cells of vertebrates.

A fine structural analysis of the fully differentiated larval caudal muscle cells of *Distaplia occidentalis* constituted the initial report in this series (Cavey and Cloney, '72). The two larval muscle bands are each composed of about 750 flattened cells arranged in longitudinal rows between the epidermis and the notochord. In each cell, a single nucleus resides in the endoplasm along with numerous mitochondria, a small Golgi body, putative primary lysosomes, proteid-yolk inclusions, and large amounts of glycogen. Myofibrils and the sarcoplasmic reticulum are confined to the peripheral sarcoplasm. The myofibrils are discrete along most of their length but branch near the tapered ends of the cell, producing a *Felderstruktur* or field of myofilaments. Myofibrils originate and terminate at specialized intercellular junctional complexes oriented orthogonally to their primary axes. A T-tubular system is absent, but numerous peripheral couplings between the sarcolemma and cisternae of the sarcoplasmic reticulum are present on all cellular surfaces. Cisternae coupled to the sarcolemma are continuous with transverse collars of sarcoplasmic reticulum which encircle the myofibrils at each I-band and H-band. Two or three longitudinal tubules are confluent with consecutive transverse collars.

The fine structure of the caudal muscle

cells in six embryonic stages of development of *Distaplia occidentalis* is described in this report. In an attempt to quantify the cellular differentiation observed on the levels of the light and electron microscopes, morphometric analyses of the volumes occupied by the major classes of organelles are provided.

Special attention is given to the assembly of myofibrils, the differentiation of transverse myomuscular junctions, the investment of myofibrils by sarcoplasmic reticulum, the formation of peripheral couplings, and the elaboration of close junctions between sarcolemmata.

MATERIALS AND METHODS

Specimens and cultures

Colonies of *Distaplia occidentalis* Bancroft (1899) were collected from the floating docks at Snug Harbor, San Juan Island, Washington, and maintained in running sea water aquaria at the Friday Harbor Laboratories of the University of Washington. Embryos in all stages of development were obtained by gently shredding a colony with forceps in a culture dish containing filtered sea water. Embryos released from torn brood sacs were washed two or three times with Millipore-filtered sea water to remove the debris from the operation. The culture dish was floated in the aquarium or held on ice until the embryos were used.

Swimming tadpoles that had escaped from mature colonies were pipetted from the aquaria directly into the fixative solutions.

To obtain a timetable for embryonic development, 24 cultures containing single embryos were established in polyethylene chambers and maintained at $13 \pm 1^\circ\text{C}$.

Millipore-filtered sea water containing 250 mg of streptomycin sulfate B per liter was used as the culture medium. The culture medium in the chambers was changed once daily. Five culture chambers contained un-cleaved eggs excised from brood sacs to insure that they were fertilized, and the remainder contained embryos of various ages.

Preparation of specimens and microscopy

Specimens were fixed with one of two fixative combinations: (1) 2% osmium tetroxide buffered by 1.25% sodium bicarbonate at pH 7.2 or 7.4 for one hour in an ice bath (Wood and Luft, '65) or (2) 2% glutaraldehyde in 0.2 M sodium cacodylate buffer (adjusted to 870 or 960 milliosmols with sucrose and containing 50 parts per million of unpurified ruthenium red) at pH 7.4 or 7.6 for three to six hours at room temperature (Cavey and Cloney, '72), followed by postfixation with bicarbonate-buffered osmium as specified above.

Following fixation with osmium, the specimens were rinsed in distilled water, dehydrated in a graded series of ethanol at room temperature, transferred through propylene oxide, and embedded in Epon (Luft, '61).

All embryos and larvae were carefully oriented on aluminum slugs before sectioning. One-micron sections for light microscopy were cut with glass knives on a Porter-Blum MT-1 ultramicrotome. Sections were stained with a mixture of azure II and methylene blue in 0.5% sodium borate (Richardson et al., '60) or with the periodic acid-Schiff (PAS) reaction after removal of the epoxy resin (Cavey and Cloney, '72). All sections were mounted in high-viscosity immersion oil.

Sections for electron microscopy were cut with a Du Pont diamond knife on a Porter-Blum MT-2B ultramicrotome at thicknesses of 400–700 Å, as judged from the interference colors of the sections. Sections were collected on 200- and 300-mesh grids or on Parlodion-supported, carbon-coated 75- or 100 × 300-mesh grids. Serial thin sections, when necessary for interpretation of the tissue, were cut at thicknesses of 700–900 Å and transferred to carbon-coated 75-mesh grids (etched with concentrated nitric acid to reduce the diameter of the grid bars) or slot grids. Thin sections were doubly stained for three

to five minutes each in aqueous solutions of uranyl acetate and lead citrate (Reynolds, '63) at room temperature.

Ultrastructural demonstration of glycogen in thin sections was achieved with the periodic acid - thiosemicarbazide - osmium (PATO) staining method, adhering to the recommendations of Vye and Fischman ('71). Only glycogen was stained by this method, and it could be enzymatically extracted from the sections by incubation in crude α -amylase at 37°C for three hours following the brief oxidation in the periodic acid. The specificity of the method was also evaluated with incomplete staining reactions: (1) distilled water was substituted for the 1% aqueous periodic acid and (2) 25% acetic acid was substituted for the 1% thiosemicarbazide in 25% acetic acid. Glycogen granules were also distinguished from ribosomes in thin sections stained only with uranyl acetate. Since glycogen is intensely stained by the lead hydroxide (Revel et al., '60) or lead citrate (Reynolds, '63) used as a counterstain to uranyl acetate, omission of the lead stain resulted in the glycogen granules being less electron dense than the intermingled ribosomes.

Electron micrographs were made with a Philips EM 300 electron microscope operated at 60 KV. The electron microscope was calibrated with a carbon grating replica of 28,800 lines/inch.

Measurements of cellular dimensions

Measurements of cellular height and width were assembled exclusively from light micrographs of transverse (1 μ) sections. Measurements of cellular length were collected from light and electron micrographs of thick (1 μ) and thin (600 Å) sections, respectively. In cells with formed myofibrils, sections were selected in which the myofibrils spanned the entire length of the cell without leaving the plane of section. The distance between the terminal transverse cellular boundaries was measured, and the accuracy of the measurements was checked against the same distances measured on electron micrographs of low magnification. The mean values from the two sources are similar. In myoblasts and differentiating muscle cells that have no myofibrils or incompletely formed myofibrils, greater reliance had to be placed

on the accurate orientation of the specimen on the microtome slug. Wide extracellular spaces between myoblasts and differentiating caudal muscle cells assisted in making accurate measurements from the light micrographs.

The cytoplasmic volume of presumptive or definitive muscle cells was calculated from the mean values of cellular length, height, and width as determined above. The mean lengths obtained from the electron micrographs were used in the calculations since higher magnification and better resolution were afforded. It was assumed that the cells have rectilinear proportions so that a simple mathematical equation ($\text{Volume} = \text{Length} \times \text{Height} \times \text{Width}$) could be used to calculate volume. In cells with slightly irregular surfaces, the assumption of rectilinearity introduces no serious error into the computations. If, however, the cells are assuming the truncated, laterally flattened, fusiform shape of the fully differentiated caudal muscle cell (Cavey and Cloney, '72), the assumption of rectilinearity results in the calculated volumes being larger than the true cellular volumes, and the error is progressively greater as the final differentiated state is attained.

Calculations of organellar volumes

Organelles change in number, relative size, and distribution in the seven stages of caudal myogenesis examined. Change in number and change in relative size are reflected in the percentage of the cellular volume which is occupied by each class of organelles. Knowing the approximate number and the general distribution of an organelle, the volume of cytoplasm occupied can be calculated with standard mathematical formulae for the volumes of spheres, hemispheres, ellipsoids, solid cylinders, and hollow cylinders. The total volume occupied by each class of organelles can then be expressed as a percentage of the total volume occupied by all classes of organelles in order to compare cells in different stages of myogenesis. (The total volume occupied by all classes of organelles and the ground cytoplasm should be comparable to the cellular volume which was calculated from the mean values of cellular length, height, and width.)

The mean size and approximate number of organelles were determined from electron micrographs of low magnification prepared for each stage of cellular differentiation. The following considerations were taken into account:

1. Discrete, membrane-bounded organelles (nucleus, mitochondria, yolk granules, lysosomes, and endoplasmic and sarcoplasmic reticula) with no intervening ground cytoplasm permit the most accurate estimations of volume.

2. Non-discrete organelles (myofibrils and Golgi apparatus) have intervening ground cytoplasm. The excess volume was excluded by multiplying the uncorrected volume by a factor representing the fraction of cytoplasm actually occupied. Correction factors were obtained from electron micrographs of higher magnification than those used to make the original estimation of volume. Excess cytoplasm contained within the organelles was tabulated in the category *ground cytoplasm*. The correction factor for the myofibrils was 0.4, and the correction factor for the Golgi apparatus was 0.5.

3. Particulate organelles (nucleolus, free and bound ribosomes, and glycogen particles) are dispersed in nucleoplasm or ground cytoplasm. Correction factors were obtained from electron micrographs where the concentration of particles per unit area could be adequately assessed. After multiplication of the uncorrected volumes by the correction factors, the excess volume dispersed among the ribosomes and glycogen granules was added to the category *ground cytoplasm*, and the excess nucleoplasm in the nucleolus was added to the volume of the nucleus. Correction factors for the particulate organelles are dependent on the stage of caudal myogenesis under consideration: nucleolus — 0.7 for stage I, 0.6 for stages II–IV, and 0.8 for stages V–VII; ribosomes — 0.1 for stages I–IV and VI–VII and 0.2 for stage V; and glycogen granules — 0.0 for stages I–II, 0.1 for stage III, 0.2 for stage IV, 0.7 for stage V, and 0.8 for stages VI–VII. (For a description of the seven embryonic and larval stages of development, designated by Roman numerals in the preceding list, consult the following subsection on embryology.)

OBSERVATIONS

Embryology

Embryos of *Distaplia occidentalis* develop within a specialized brood sac that appears as a posterior outgrowth of the atrial cavity of the reproductive zooid (Bancroft, 1899). A timetable of embryonic development under controlled temperature is presented in table 1, where those stages contributing to this study of caudal myogenesis are designated by Roman numerals (I-VII). A brief description of each of the seven stages follows.

Neurulating embryo: Stage I of caudal myogenesis (fig. 10)

The neural groove of the neurulating embryo is closed anteriorly, and the presumptive muscle cells (myoblasts) are segregated into two bands beneath the epidermis in the caudal rudiment.

Caudate embryo: Stage II of caudal myogenesis (fig. 12)

The neural groove of the caudate embryo is completely closed and the myoblasts are dividing, as determined from the mitotic division figures seen in thick Epon sections

under the compound microscope. The length of the tail is less than one-third the circumference of the trunk. The trunk superficially appears undifferentiated, but paired ectodermal sacs (rudiments of the peribranchial cavities) are present.

Comma embryo: Stage III of caudal myogenesis (fig. 14)

The length of the tail of the comma embryo is one-third to one-half the circumference of the trunk. The frequency of mitotic division figures among the muscle-forming cells is very low. The elongating tail is situated in a shallow ventral groove of the trunk. The developing notochord is allanoid in form and composed of an aggregation of discoidal cells.

Vesiculate embryo: Stage IV of caudal myogenesis (fig. 19)

The two muscle bands of the vesiculate embryo are approximately two-thirds of their final length. The tail begins a 90° rotation at its base, reorienting the dorsal caudal tissues to the left side of the trunk and the ventral caudal tissues to the right side. Intercellular accumulations of matrix appear between the notochordal cells, marking the onset of the transition of the notochord from a column of discoidal cells into a hollow supportive cylinder (Cloney, '64). There is ultrastructural evidence for the initial deposition of tunic on the apical surfaces of the epidermal cells. An indentation marking the position of the future sensory vesicle is located in the posterodorsal region of the trunk.

Papillate embryo: Stage V of caudal myogenesis (fig. 23)

The notochord of the papillate embryo is a hollow cylinder. In the trunk, the nascent adhesive papillae are prominent, the ocellus and otolith are differentiating in the sensory vesicle, and the primordia of the paired atrial siphons and the single branchial siphon become elevated. Test cells, released from the cortical ooplasm into the perivitelline space after fertilization, are found in close contact with the tunic. The test cells apparently secrete granules which ornament the surface of the larval tunic (M. J. Cavey and R. A. Cloney, unpublished observations).

TABLE 1

Timetable of embryonic development at 13 ± 1 °C for Distaplia occidentalis

Stage of embryogenesis	Time (hrs)	Range (hrs)	No. of cultures
Uncleaved egg	0	—	5
Two cells	26	—	4
Four cells	52	52—53	4
Eight cells	79	77—84	5
Sixteen cells	105	103—111	6
Early blastula	132	130—139	5
Late blastula	159	155—168	5
Early gastrula	183	179—192	3
Mid-gastrula	209	205—219	3
Late gastrula	236	232—246	4
Neurulating embryo (I)	256	251—267	3
Caudate embryo (II)	282	277—294	7
Comma embryo (III)	332	324—348	10
Vesiculate embryo (IV)	381	370—399	11
Papillate embryo (V)	453	442—471	11
Prehatching tadpole (VI)	581	566—603	9
Swimming tadpole (VII)	664	647—687	6

Prehatching tadpole: Stage VI of caudal myogenesis (fig. 30)

Contractions of the caudal muscle bands are pronounced and may assist the prehatching tadpole in breaking out of the chorion when ready to hatch. The rudiment of the branchial basket is perforated, and an endostyle is located along the future ventral side of the basket. The alimentary tract is fully differentiated, and the heart contracts rhythmically near the loop of the intestine. A posterior cavity in the trunk is formed and will receive the axial complex (muscle bands, notochord, nerve cord, and endodermal strand) when the swimming tadpole undergoes metamorphosis (Cloney, '72).

Swimming tadpole: Stage VII of caudal myogenesis

Upon hatching, the swimming tadpole possesses two fully differentiated bands of caudal muscle, one on each side of the notochord. A fine structural examination of the caudal muscle cells (Cavey and Cloney, '72) and detailed descriptions of the other caudal tissues (Cloney, '72) are provided elsewhere.

Hereafter, the embryonic or larval nomenclature will be followed by parenthetical Roman numerals indicating the stage of caudal myogenesis.

Changes in cellular dimensions and volume

The dimensions of the presumptive and definitive caudal muscle cells were obtained from light and electron micrographs of thick- and thin-sectioned tissue. The measurements and statistical analyses of them are presented in table 2. Data on the fully differentiated caudal muscle cells of the swimming tadpole (VII) are tabulated elsewhere (Cavey and Cloney, '72).

Myoblasts of the neurulating embryo (I) have similar heights and similar widths regardless of position within the presumptive muscle bands. The ratio of mean cellular height to mean cellular width (H/W) is 3.3:1. Myoblasts of the caudate embryo (II) also have similar heights and similar widths regardless of position within the bands. The ratio of mean height to mean width averages 3.8:1, and the increased height reflects the movement of myoblasts into positions permitting them to contact both the epidermal and the notochordal

boundaries of the presumptive muscle bands. The cellular length diminishes somewhat in comparison with myoblasts of the neurulating embryo (I).

A difference between cells in the dorsal- or ventral-most part of the muscle bands and the cells in the medial region of the bands is first noticed in the measurements of cells of the comma embryo (III). The height of the medial cells (H/W = 3.9:1) is greater than the height of the dorsal or ventral cells (H/W = 2.6:1); conversely, the width of the medial cells is less than that of the dorsal or ventral cells. The cellular length is essentially unchanged in comparison with myoblasts of the caudate embryo (II). The difference in mean dimensions is further expressed in muscle cells of the vesiculate embryo (IV). The dorsal and ventral cells of the muscle bands are more flattened (H/W = 5.2:1) than the medial cells (H/W = 2.6:1), and the cellular length has doubled.

In muscle cells of the papillate embryo (V), the ratios of height to width for the dorsal and ventral cells (5.0:1) and for the medial cells (2.4:1) have slightly diminished, but the cellular length has marginally increased. Muscle cells of the prehatching tadpole (VI) are unchanged in length, but the height to width ratios for the dorsal and ventral cells (5.3:1) and for the medial cells (1.9:1) continue to diverge.

The fully differentiated muscle cells of the swimming tadpole (VII) are longer than the cells of the prehatching tadpole (VI). The dorsal and ventral cells still exhibit a moderately large height to width ratio (3.3:1), while the ratio for the medial cells (0.9:1) becomes less than unity.

It is possible to calculate the mean cellular volume at each stage of caudal myogenesis by using the mean cellular dimensions given in table 2 and by assuming that the cells have rectilinear proportions (table 3). The mean cellular volume is plotted as a function of the stage of caudal myogenesis (embryonic age) in figure 1. The mean volume declines from stage I to stage III. The time span encompassed by these stages is a period of mitotic activity, and a decrease in volume would be expected. The mean cellular volume increases between stage III and stage IV, and there are small increases in volume in successive stages. Although the small increases in volume

TABLE 2

Dimensions of differentiating caudal muscle cells

All cells:						
Length ¹	I	Neurulating embryo	13.0	± 1.5	10.8–16.3	50
	II	Caudate embryo	9.3	± 1.1	7.6–12.3	50
	III	Comma embryo	10.5	± 1.1	8.1–12.8	50
	IV	Vesiculate embryo	19.2	± 2.1	14.9–27.6	50
	V	Papillate embryo	25.0	± 2.2	14.2–32.3	50
	VI	Prehatching tadpole	22.9	± 2.0	13.4–27.8	50
Length ²	I	Neurulating embryo	12.2	± 1.1	10.7–14.9	50
	II	Caudate embryo	9.7	± 0.7	8.2–11.2	50
	III	Comma embryo	9.1	± 0.8	8.2–10.2	50
	IV	Vesiculate embryo	21.3	± 0.8	19.1–22.7	50
	V	Papillate embryo	23.1	± 0.7	21.7–26.2	50
	VI	Prehatching tadpole	22.1	± 0.5	21.4–24.3	50
Dorsal and ventral cells:						
Height ³	I	Neurulating embryo	32.4	± 1.5	28.5–34.3	50
	II	Caudate embryo	37.2	± 1.0	31.6–39.6	50
	III	Comma embryo	20.3	± 1.6	17.3–25.4	50
	IV	Vesiculate embryo	22.2	± 1.9	20.2–24.9	50
	V	Papillate embryo	21.5	± 1.2	17.4–25.0	50
	VI	Prehatching tadpole	23.4	± 1.7	18.8–27.0	50
Width ³	I	Neurulating embryo	9.9	± 1.4	7.7–13.2	50
	II	Caudate embryo	9.9	± 1.2	7.8–12.4	50
	III	Comma embryo	7.7	± 1.4	4.0–10.4	50
	IV	Vesiculate embryo	4.3	± 0.8	3.4– 6.4	50
	V	Papillate embryo	4.3	± 0.2	2.2– 4.6	50
	VI	Prehatching tadpole	4.4	± 0.2	3.8– 5.9	50
Medial cells:						
Height ³	I	Neurulating embryo	32.2	± 1.4	28.9–34.8	50
	II	Caudate embryo	9.6	± 1.2	7.6–12.5	50
	III	Comma embryo	6.2	± 1.6	2.7– 9.3	50
	IV	Vesiculate embryo	6.1	± 0.8	4.7– 7.9	50
	V	Papillate embryo	6.2	± 0.3	3.9– 7.5	50
	VI	Prehatching tadpole	7.2	± 1.5	4.7–11.1	50

¹ Measurements from light micrographs of longitudinal sections.² Measurements from electron micrographs of longitudinal sections.³ Measurements from light micrographs of transverse sections.

from stage IV through stage VII may be real, they could also be accounted for by the error introduced into the calculations by the assumption that cells have rectilinear proportions. The assumption is most applicable to cells in stages I–III. In later stages, each cell assumes the shape of a flattened, truncated spindle with stepped, subterminal surfaces (Cavey and Cloney, '72), and the assumed rectilinearity introduces progressively greater amounts of error into the calculations as the final state

of differentiation is attained. There may be no significant change in cellular volume from stage IV to stage VII.

*Changes in cellular shape, position,
and distribution of
organelles*

Neurulating embryo (I) (figs. 2, 11)

The myoblasts of the neurulating embryo are situated in two bands composed of two or three layers. The bands, enveloped

TABLE 3

Volumes of differentiating caudal muscle cells^{1,2}

Stage	Description	Mean volume (μ^3)	Range (μ^3)
Dorsal and ventral cells			
I	Neurulating embryo	3913	2915-5095
II	Caudate embryo	3572	2834-4410
III	Comma embryo	1422	978-1973
IV	Vesiculate embryo	2033	1457-2716
V	Papillate embryo	2136	1864-2431
VI	Prehatching tadpole	2275	1969-2609
Medial cells			
I	Neurulating embryo	3811	2872-4916
II	Caudate embryo	3455	2706-4313
III	Comma embryo	1365	882-1796
IV	Vesiculate embryo	2092	1684-2533
V	Papillate embryo	2077	1797-2382
VI	Prehatching tadpole	2212	1514-3028

¹ Mean cellular dimensions from table 2 were substituted into the equation for the volume of a regular solid (Volume = Length \times Height \times Width). The possible error introduced into the calculations by the assumption of rectilinearity is discussed in the text.

² The range of cellular volumes within one standard deviation on either side of the mean cellular dimensions (table 2) is displayed.

by an external lamina, flank the notochord and lie beneath the yolky epidermal cells of the caudal rudiment. All cells have a low columnar profile, and the plasmalemmata are moderately convoluted. Small junctional complexes, unique to the mitotic myoblasts and structurally dissimilar to the close junctions between definitive caudal muscle cells, are observed between the plasmalemmata of apposed digitate filopodia from adjacent cells. Proteid-yolk granules of variable size and shape occupy most of the cellular volume, displacing the nucleus to the peripheral cytoplasm. The large spherical nucleus has a fine layer of condensed chromatin on the inner membrane of its envelope. Annulate lamellae and three or four prominent nucleoli are dispersed in the nucleoplasm. The cytoplasmic surface of the outer membrane of the nuclear envelope is studded with polysomes, and evaginations of this membrane are continuous with cisternae of rough-surfaced endoplasmic reticulum (ER). A few small mitochondria with simple cristae lie subadjacent to the nucleus and in the ground cytoplasm between the yolk granules. Two or three Golgi bodies, each consisting of four to seven flattened cisternae, commonly occur; the forming faces are usually direct-

ed toward the nucleus, but there are no visible secretory granules. The ground cytoplasm contains a minute amount of glycogen and a moderate number of free ribosomes and polysomes. A pair of centrioles is typically located either in a small cellular outpocketing near the nucleus or between the nucleus and one of the Golgi bodies.

Caudate embryo (II) (figs. 3, 13)

The myoblasts of the caudate embryo undergo mitotic divisions and become reoriented so that each cell adjoins both the epidermis and the notochord. Many slender filopodia extend from the myoblasts as they become rearranged within the presumptive muscle bands; microtubules in the filopodia lie parallel to the axis of cellular elongation. As the myoblasts assume a tall columnar configuration, numerous junctional complexes typifying the presumptive caudal muscle cells arise between the convoluted plasmalemmata. Like the myoblasts of the neurulating embryo (I), proteid-yolk granules occupy a major portion of the cellular volume. The ovoid nucleus is displaced either toward the epidermal or toward the notochordal pole of the cell by the yolk inclusions. Three or four nucleoli and long segments of annulate lamellae are observed in the nucleoplasm. The ongoing evagination of the nuclear envelope produces a perinuclear zone of rough-surfaced ER. A few mitochondria are situated near the nucleus; these organelles have grown slightly in diameter but have not changed in their ultrastructural complexity. The presence of electron dense material in the cisternae, vesicles, and associated vacuoles of the Golgi bodies indicates that the organelles are active in synthesis. The forming faces of the Golgi bodies are randomly directed. The first indications of the degradation of yolk granules coincide with the signs of secretory activity in the Golgi bodies. The ground cytoplasm contains little glycogen, except in regions immediate to degrading proteid-yolk granules. The concentration of free ribosomes and polysomes is increasing.

Comma embryo (III) (figs. 4, 15)

After adjoining the boundaries of the epidermis and the notochord, the differentiating muscle cells of the comma embryo

begin to elongate parallel to the long axis of the tail. The plasmalemmata, now appropriately called the sarcolemmata, are irregularly infolded but to a lesser degree than in myoblasts of either the neurulating embryo (I) or the caudate embryo (II). A few close junctions join abutting muscle cells. Proteid-yolk reserves are greatly depleted, and the remaining yolk granules are restricted to the apical and basal parts of a cell. The nucleus assumes a central position within the sarcoplasm, and its envelope becomes indented. Annulate lamellae disappear from the nucleoplasm, and only one or two nucleoli remain. Mitochondria are widely dispersed throughout the sarcoplasm, and their cristae begin to anastomose. A single Golgi body (occasionally two) is situated close to the nucleus and directed away from it. The Golgi body is actively engaged in packaging secretory granules, and numerous granules lie in proximity to the remaining yolk granules. With no indications of exocytosis, the secretory granules may be primary lysosomes; such granules will hereafter be referred to as *putative primary lysosomal (PPL) granules*. The degradation of yolk granules parallels the increase of glycogen in the ground sarcoplasm, but free and bound ribosomes still predominate.

Thick and thin myofilaments (presumably myosin and actin filaments) are synthesized in the peripheral sarcoplasm. Although joined to each other, the thick and thin myofilaments display no sarcomeric bands. Networks of myofilaments occur in random orientations.

Rough-surfaced sarcoplasmic reticulum (SR) resides in the central region of a cell, and short segments of it are also common in the peripheral sarcoplasm within the differentiating field of myofilaments. Intimate associations (peripheral couplings) between the sarcolemma and cisternae of smooth-surfaced SR (subsarcolemmal cisternae) are established. Cisternae in close association with the sarcolemma are devoid of ribosomes, however segments farther removed may retain them.

Vesiculate embryo (IV) (figs. 5, 20)

The differentiating muscle cells of the vesiculate embryo are enlarging. The height and width of the cells are about equivalent to those of the comma embryo (III), but the

cellular length has doubled. As cells begin to assume their definitive configuration, the terminal cellular boundaries of neighboring cells interdigitate, possibly as a prelude to the establishment of the stepped, subterminal, lateral cellular surfaces characteristic of the fully differentiated caudal muscle cells (Cavey and Cloney, '72). Apposed sarcolemmata are separated by a slightly irregular extracellular space. Close junctions proliferate and grow in circumference, and the separation between sarcolemmata is constant in these regions. The fine layer of condensed chromatin beneath the inner membrane of the nuclear envelope and one or two nucleoli are retained. Yolk reserves of the cell are contained within a few massive granules and numerous smaller granules dispersed in the ground sarcoplasm. Mitochondria exhibit an increasingly complex pattern of anastomosing cristae, and each cell contains a single, synthetically active, Golgi body whose forming face is directed toward the nascent field of myofilaments in the peripheral sarcoplasm. The number of PPL granules in the vicinity of the Golgi body and in the proximity of the remaining yolk granules is noticeably larger than in the preceding stages of caudal myogenesis. Continued degradation of proteid-yolk is associated with the increase of glycogen in the sarcoplasm. Glycogen granules are usually discrete, but some are aggregated into rosettes. Free ribosomes and polysomes remain plentiful.

The striking feature of the muscle cell is the differentiating field of myofilaments. The networks of myofilaments are joined end-to-end and oriented roughly parallel to the long axis of the cell, a short distance beneath the sarcolemma. The orderly arrangement of myofilaments coincides with the appearance of precursory Z-lines which demarcate the sarcomeric I-bands. The alignment of overlapping thick and thin myofilaments in the A-band is insufficient to clearly delimit either the H-band or the M-line. Additional thick and thin myofilaments are added to the periphery of the myofibrils which span the entire length of the cell. There is no evidence of the formation of transverse myomuscular junctions. Thin myofilaments from the terminal sarcomeres frequently contact the sarcolemma.

Membranes of the sarcoplasmic reticulum in the peripheral sarcoplasm bear few attached ribosomes. Rough-surfaced SR is prevalent in the endoplasm. The arrangement of sarcoplasmic reticulum in the differentiating field of myofilaments is unordered, but peripheral couplings between the sarcolemma and cisternae of SR continue to form. Peripheral couplings are restricted to stretches of the sarcolemma not involved in the formation of close junctions.

Papillate embryo (V) (figs. 6, 24, 27)

The subterminal, lateral surfaces of the differentiating muscle cells of the papillate embryo are forming into steps which will be the loci of the transverse myomuscular junctions. The cellular length, height, and width are essentially unchanged in comparison with the cells of the vesiculate embryo (IV). The sarcolemmata are nearly parallel to each other, and close junctions in various stages of differentiation are found between membranes of laterally apposed cells. An irregularly indented, elongate nucleus with only a single nucleolus occupies the central endoplasm; numerous PPL granules are scattered among the few remaining yolk inclusions. A single Golgi body, situated close to the nucleus, is directed toward the peripheral field of myofilaments. Large mitochondria of irregular diameter occupy a greater portion of the cellular volume, and they are characterized by serpentine anastomosing cristae. Small, localized accumulations of glycogen granules and of ribosomes impart a patchy appearance to the ground sarcoplasm. The glycogen granules are aggregated into small rosettes and occupy a volume that is almost equivalent to that occupied by the ribosomes.

A new feature of the field of myofilaments is the presence of myomuscular junctions at the transverse cellular boundaries on the lateral, subterminal and terminal surfaces. The orientation of many of these junctions is initially oblique to the primary axes of the myofibrils. Better alignment of the overlapping thick and thin myofilaments in the A-bands produces distinct H-bands and M-lines.

The amount of rough-surfaced SR is declining, especially from the endoplasm. Reticular membranes in the peripheral sarcoplasm are almost entirely smooth-sur-

faced. The sarcoplasmic reticulum begins to invest the myofibrils. A single, perforated sheet of SR, centered on the Z-line and extending laterally to the boundaries with the A-band, is detectable. A second sheet, centered on the M-line and embracing the H-band, is beginning to envelop the center of the sarcomere. Peripheral couplings are usually situated closer to the Z-lines than to the M-lines, indicating a temporal separation between formation of the reticular collars in the two sarcomeric positions.

Prehatching tadpole (VI) (figs. 7, 31, 38)

The muscle cells of the prehatching tadpole have stepped, subterminal, lateral surfaces that are nearly identical to those of cells in the swimming tadpole (VII). The cellular dimensions are comparable to those of the papillate embryo (V). Close junctions between sarcolemmata continue to differentiate. The elongate nucleus frequently abuts on the sarcolemma; a single, bipartite nucleolus is contained in the nucleoplasm. The polysomes bound to the outer membrane of the nuclear envelope began to disappear in the papillate embryo (V), and their loss from the envelope is now almost complete. The remaining proteid-yolk granules are in various stages of degradation. A synthetically active Golgi body is associated with each muscle cell of the prehatching tadpole and the swimming tadpole (VII). Additional degradation of yolk enhances the patchy appearance of the ground sarcoplasm, and glycogen granules now occupy more of the cytoplasmic volume than do the ribosomes. Glycogen particles are aggregated into multigranular rosettes. Large mitochondria are excluded from the peripheral sarcoplasm by the myofibrils and are arranged in one to three, closely packed layers in the endoplasm.

Myofibrils of the peripheral field have well defined sarcomeric bands. Investment of the center of the sarcomere with sarcoplasmic reticulum progresses, and a complete, although single, layer of SR overlies the H-band. Peripheral couplings near the H-bands are infrequently observed. The majority of myomuscular junctions are orthogonal to the primary axes of the myofibrils.

Swimming tadpole (VII)

For a fine structural examination of the differentiated caudal muscle cells of the

swimming tadpole and a schematic diagram of typical cells, consult Cavey and Cloney ('72).

Absolute and relative volumes of cellular organelles

The state of differentiation of the ascidian caudal muscle cells can be expressed in terms of the cytoplasmic volume that is occupied by the various classes of organelles and inclusions dispersed in ground cytoplasm. Estimations of the absolute and relative volumes of the major organelles have been calculated from electron micrographs, and the basic data for the seven stages of caudal myogenesis are contained in table 4.

The absolute cytoplasmic volume occupied by each class of organelles is plotted as a function of the stage of caudal myogenesis (embryonic age) in figure 8. The nucleus, nucleoli, ribosomes, and yolk granules decline in absolute amount as cellular dif-

ferentiation proceeds. Glycogen granules, mitochondria, and myofilaments increase in absolute amount. The endoplasmic and sarcoplasmic reticula and putative primary lysosomes rise and fall in absolute amount. Change in the absolute volume of the Golgi complex cannot be assessed from the graph because of its small volume; the absolute volume rises to a maximum in the caudate embryo (II), then declines, and is relatively constant in stages V-VII of caudal myogenesis.

Although the change in absolute volumes of organelles offers some indication of the state of cellular differentiation, it should be emphasized that the cells undergo abrupt changes in volume during the process (fig. 1, table 3). Subtle, and possibly significant, changes in the volume of organelles may be masked by the change in cellular volume. The relative amount of organelles, therefore, may provide the most reliable

TABLE 4
*Approximate cytoplasmic volume occupied by classes of organelles*¹

Class of organelles		Stage of caudal myogenesis ²						
		I	II	III	IV	V	VI	VII
Nucleus	μ^3	120	112	89	34	30	32	29
	%	2.9	3.4	7.1	1.6	1.4	1.4	1.3
Nucleolus	μ^3	22	15	15	4	5	2	2
	%	0.5	0.5	1.2	0.2	0.2	0.1	0.1
Mitochondria	μ^3	92	51	33	437	678	802	786
	%	2.1	1.5	2.6	20.8	31.1	34.7	35.6
Myofilaments	μ^3	0	0	21	203	406	491	459
	%	0.0	0.0	1.7	9.6	18.6	21.2	20.8
Yolk inclusions	μ^3	2346	1384	280	102	32	14	4
	%	55.8	41.6	22.3	4.8	1.5	0.6	0.2
Golgi apparatus	μ^3	1	1	1	0	0	0	0
	%	0.0	0.0	0.0	0.0	0.0	0.0	0.0
Endoplasmic reticulum	μ^3	84	176	10	15	35	60	90
	%	2.0	5.3	0.8	0.7	1.6	2.6	4.1
Lysosomes	μ^3	0	0	26	24	17	12	13
	%	0.0	0.0	2.1	1.2	0.8	0.5	0.7
Glycogen	μ^3	0	0	2	18	73	68	129
	%	0.0	0.0	0.2	0.9	3.4	2.9	5.8
Ribosomes	μ^3	93	111	79	72	62	14	0
	%	2.2	3.4	6.3	3.4	2.8	0.6	0.0
Ground cytoplasm	μ^3	1451	1473	699	1197	841	816	693
	%	34.5	44.3	55.7	56.8	38.6	35.4	31.4
Totals	μ^3	4209	3323	1255	2106	2179	2311	2205
	%	100.0	100.0	100.0	100.0	100.0	100.0	100.0

¹ The absolute volume of each class of organelles is expressed in cubic microns, and the relative volume is the absolute volume of each class of organelles expressed as the percentage of the total cytoplasmic volume occupied by all classes of organelles.

² Roman numerals designate each stage of caudal myogenesis and the appropriate embryo or larva: I, Neurulating embryo; II, Caudate embryo; III, Comma embryo; IV, Vesiculate embryo; V, Papillate embryo; VI, Prehatching tadpole; VII, Swimming tadpole.

information. The percentage of the cytoplasmic volume occupied by each class of organelles has also been calculated (table 4) and is plotted as a function of the stage of caudal myogenesis (embryonic age) in figure 9. Several correlations can be made from these data. A striking change occurs in the relative amount of yolk in cells during the first half of differentiation. Since the degradation of yolk may be responsible for the production of glycogen, the declining content of yolk correlates with the rising content of glycogen. In addition, the content of putative primary lysosomes is maximal during the most active periods of degradation of yolk and then declines gradually as the yolk reserves are expended.

The ratio of nuclear volume to cytoplasmic volume is greatest in the caudal muscle cells of the comma embryo (III), and the same relationship holds for the nucleolar component. The rise in prominence of the nucleolar component is paralleled by the rising content of ribosomes. (In the comma embryo (III), ribosomes are required for the synthesis of myofilaments; as the assembly of myofibrils proceeds, the need for ribosomes and the nucleoli to produce them lessens.) From calculations of the mean cellular volume during differentiation (fig. 1), it appears that the cellular volume is essentially the same for cells in stages IV–VII of caudal myogenesis, and the constant cytoplasmic volume is also reflected in an unchanging nuclear volume: the nuclear to cytoplasmic ratio is constant.

The amount of endoplasmic and sarcoplasmic reticula exhibits a bimodal distribution. One maximum occurs early in differentiation in the caudate embryo (II) and reflects the production of rough-surfaced endoplasmic reticulum by evagination of the nuclear envelope. A second maximum is gradually attained at the end of differentiation and represents the smooth-surfaced sarcoplasmic reticulum that invests the myofibrils and is probably responsible for coupling the events of excitation of the sarcolemma and contraction of the myofibrils.

The increase in the relative volume of myofilaments and mitochondria as cells attain progressively more differentiated states is characteristic of fast-acting skeletal muscle cells in general. Very few attempts have been made, however, in other systems to

quantify the content of organelles in cells studied with the electron microscope (Luff and Atwood, '71; Peachey, '65).

Differentiation of the contractile apparatus

Thick (presumably myosin) and thin (presumably actin) myofilaments appear simultaneously in the peripheral sarcoplasm of cells of the comma embryo (III) (fig. 15). Individual myofilaments are interspersed among the polysomes in the peripheral sarcoplasm, and a few are occasionally observed deep in the endoplasm. Networks of loosely aligned myofilaments lie parallel to the sarcolemma but are randomly oriented with respect to the principal axes of the cell. The alignment of myofilaments within the networks is achieved by the formation of bridges between the thick and thin myofilaments (fig. 16) and by the formation of bridges between the naked central shafts of the thick myofilaments (fig. 17). The myofilaments are hexagonally packed, and the pattern resembles the one observed in the fully differentiated sarcomeres of the swimming tadpole (VII) (Cavey and Cloney, '72). Both types of myofilament are present in the networks, but a full complement of thin myofilaments (six thin myofilaments surrounding each thick myofilament) was never observed (fig. 16). It is inferred that the thick myofilaments initially associate by H-bridges interconnecting their central shafts and that the thick and thin myofilaments secondarily associate by actomyosin bridges.

The thin myofilaments have a diameter of 50–55 Å, and the thick myofilaments have a diameter of 110–130 Å. Both types of myofilament are sometimes as long as the myofilaments in the fully differentiated sarcomeres of the swimming tadpole (VII), but shorter myofilaments are more frequently observed. There can be no reliable measurements of length because the myofilaments often diverge from the plane of section. No sarcomeric banding pattern is evident in the networks of myofilaments, even though the formation of H-bridges should delimit an M-line.

The networks of myofilaments orient roughly parallel to the long axis of the muscle cell of the vesiculate embryo (IV) and become restricted to the peripheral

sarcoplasm (figs. 20, 21). Thick myofilaments in the core of a growing network possess a full complement of thin myofilaments. The networks span the entire length of the cell and increase in diameter by appositional growth. Precursory Z-lines between successive networks of myofilaments appear to interact with the thin myofilaments to form the nascent Z-lines. The A-bands still do not have distinct H-bands or M-lines, but the indistinctly demarcated A-bands and I-bands are often in register across sarcolemmata.

The muscle cells of the papillate embryo (V) contain a well differentiated row of cortical myofibrils. The thick and thin myofilaments of the A-bands are more precisely ordered, and definite H-bands and M-lines are present (fig. 24). The morphology of the Z-lines continues to be nondiscoidal. Amorphous material associated with the I-bands obscures the thin myofilaments and Z-filaments. The amorphous material is concentrated over the thin myofilaments in two zones, one on either side of the Z-line, in adjacent sarcomeres.

In muscle cells of the prehatching tadpole (VI), the irregularities in the architecture of the Z-lines have disappeared, and the Z-lines become discoidal. I-bands are moderately distinct, and the amorphous material dispersed among the thin myofilaments is concentrated over the Z-lines (fig. 31).

Differentiation of the transverse myomuscular junctions

At the terminal and subterminal, transverse boundaries of the caudal muscle cells of the swimming tadpole (VII), myofibrils insert into specialized intercellular junctional complexes oriented orthogonally to the primary axes of the myofibrils and superficially resembling the intercalated disks of vertebrate cardiac muscle. To denote their presence in somatic striated muscle and to distinguish them from other junctional complexes between cells, they have been referred to as *transverse myomuscular* (TMM) *junctions* (Cavey and Cloney, '72).

There is no evidence of the formation of transverse myomuscular junctions between muscle cells of the comma embryo (III) or the vesiculate embryo (IV), although these

two stages of caudal myogenesis are characterized by either networks of myofilaments or by nascent myofibrils with incompletely banded sarcomeres. In the vesiculate embryo (IV), thin myofilaments from the terminal sarcomeres closely approach and frequently contact the sarcolemma at the transverse cellular boundary, but the only specialized contacts between the sarcolemmata are close junctions (fig. 21).

In the papillate embryo (V), orthogonally and obliquely oriented myomuscular junctions occur. Individual myofibrils insert at a myomuscular junction at the level of a sarcomere corresponding to a Z-line (fig. 25). Several myofibrils may insert at a single myomuscular junction and, conversely, a single myofibril may split and insert at more than one junction. At the region of juncture, the apposed sarcolemmata are separated by an extracellular space approximately 350 Å wide. In the extracellular junctional space, equidistant from the two parallel sarcolemmata, a dense layer of material is found (fig. 26). Extracellular thin filaments, 60–70 Å in diameter, penetrate the dense layer and traverse the space at right angles to the sarcolemmata. The terminal halves of the I-bands at the junction, as well as the other sarcomeric I-bands, are obscured by amorphous material dispersed among the thin myofilaments.

The myomuscular junctions of the prehatching tadpole (VI) are predominantly orthogonal to the primary axes of the myofibrils (fig. 32), but a few obliquely oriented junctions are often encountered (fig. 33). In the terminal halves of the I-bands at the region of juncture, amorphous material collects into a band of Z-matrix which is separated from the sarcolemma by an area of low electron density. The intracellular deposition of Z-matrix almost doubles the width of the terminal halves of the I-bands and permits the resolution of the myomuscular junctions with the compound microscope. Thin myofilaments traverse the area of low electron density and contact the sarcolemma. The myofilaments frequently appear to be aligned with the extracellular filaments in the junctional space (fig. 34). The junctional space measures 550 Å in width, comparable to the width of the space of the fully differenti-

ated TMM junction between cells of the swimming tadpole (VII), and no longer contains a central dense layer.

Differentiation of the sarcoplasmic reticulum and peripheral couplings

The sarcoplasmic reticulum establishes contact between the myofibrils and the sarcolemma in the fully differentiated caudal muscle cells of the swimming tadpole (VII). *Peripheral couplings* (terminology after Johnson and Sommer, '67) between the sarcolemma and *subsarcolemmal cisternae* (terminology after Fawcett and McNutt, '69) of SR occur on all cellular surfaces. The sarcoplasmic reticulum investing each myofibril consists of longitudinal tubules which are confluent with transverse collars encircling each I-band and H-band (Cavey and Cloney, '72).

Rough-surfaced endoplasmic reticulum derives from evaginations of the nuclear envelope of myoblasts of the neurulating embryo (I) and the caudate embryo (II). Cisternae of ER contain the same flocculent material which exists between the inner and outer membranes of the envelope (figs. 11, 13). Reticular membranes accumulate in a zone encompassing the nucleus before pervading the entire cytoplasm.

Muscle cells of the comma embryo (III) have nearly completed their mitotic divisions, and most of the 1500 cells in the two caudal bands are present. Synthesis of myofilaments and aggregation into networks are accompanied by changes in the sarcoplasmic reticulum. Reticular membranes in the peripheral sarcoplasm become increasingly free of ribosomes (fig. 15), and the nuclear envelope buds reticular membranes without ribosomes. Rough-surfaced sarcoplasmic reticulum is confined to the endoplasm, and smooth-surfaced SR establishes the first peripheral couplings with the sarcolemma. Subsarcolemmal cisternae closely approach the cellular membrane and are nearly parallel with it, but the gap of the peripheral coupling is slightly irregular in width. Parts of the subsarcolemmal cisterna that extend away from the sarcolemma can bind ribosomes (fig. 18).

Smooth-surfaced SR proliferates about the nascent myofibrils in the muscle cells of the vesiculate embryo (IV). The sarco-

plasmic reticulum bears no patterned association with the roughly demarcated bands of the sarcomere (fig. 20). The frequency of peripheral couplings increases, and paired peripheral couplings are common because the myofibrils lie in close register across sarcolemmata (fig. 22). A central dense plaque occurs in the gap of the peripheral coupling and is situated equidistant from the apposed sarcolemmal surfaces.

The sarcoplasmic reticulum becomes organized in specific patterns around the myofibrils in muscle cells of the papillate embryo (V) (figs. 24, 27). A transverse collar of SR, centered on the Z-line, completely invests each I-band (fig. 28), and peripheral couplings join it with the sarcolemma. The couplings are restricted to stretches of the sarcolemma near the I-bands. A second collar of SR, centered on the M-line, incompletely invests each H-band as a single layer (fig. 29). Regions of the sarcolemma near the H-bands rarely participate in the formation of peripheral couplings. Two or three longitudinal tubules of SR lie on the surface of the A-band between the differentiating collars in the two sarcomeric positions.

In the prehatching tadpole (VI), the morphology of the transverse collar of sarcoplasmic reticulum encircling the I-band is unchanged (figs. 31, 38). The transverse collar centered on the M-line and embracing the H-band, however, completely invests the myofibril as a single, perforated sheet (fig. 38). The sheet is discontinuous on the side of the myofibril most distant from the sarcolemma, and the free ends of the sheet frequently lift off the surface of the myofibril at the raphe and must recurve, prior to extending toward the sarcolemma and establishing peripheral couplings with it. Peripheral couplings with the sarcolemma proximal to the H-bands are uncommon, also indicative of a temporal separation between the formation of the reticular collars in the two sarcomeric positions (fig. 39).

Sarcolemmata and the differentiation of close junctions

The sarcolemmata are irregularly convoluted on all surfaces of the caudal muscle cells of the swimming tadpole (VII). Gaps between the cells are uniform only at

the transverse myomuscular junctions and at the close junctions. Close junctions are prevalent between laterally apposed cells and are interposed between regions of the sarcolemmata involved in the formation of peripheral couplings (Cavey and Cloney, '72).

Dividing myoblasts of the neurulating embryo (I) and the caudate embryo (II) establish small junctional complexes between plasmalemmata, but the morphology of these junctions is unlike that of the close junctions found between cells in later stages of caudal myogenesis. Apposed plasmalemmata are separated by a wide extracellular space that measures approximately 250 Å in width. Dense material occupies the extracellular space and is often situated in two dense layers (fig. 35). Such junctional complexes are only observed between myoblasts and never between definitive muscle cells. Since myoblasts are active in mitosis, the junctional complexes with wide extracellular spaces could be quite transitory. Similar junctional complexes with relatively wide extracellular spaces are also found between differentiating murine skeletal muscle cells (Kelly and Zacks, '69).

Close junctions typical of those between the differentiated caudal muscle cells of the swimming tadpole (VII) become numerous as the cells attain more differentiated conditions. Formation of close junctions is not a synchronous event. Parallel sarcolemmata with a uniform extracellular space signify an early stage in the formation of a close junction. Shortly after or concurrently, fibrous material appears in the space and a dense layer is deposited equidistant from both of the apposed sarcolemmal surfaces. Extracellular thin filaments, 60–70 Å in diameter, penetrate the dense layer and interconnect the two cellular membranes (fig. 37). (Almost identical events may occur during the formation of a transverse myomuscular junction.) The extracellular space is gradually obliterated until the separation of the outer leaflets of the two sarcolemmata is reduced to 30–40 Å. The image of the fully differentiated close junction is usually septilaminar (fig. 36).

The characterization of the junctional complexes between sarcolemmata in ascidian embryos and larvae is incomplete. In the absence of studies using electron-opaque

tracers and the techniques of freeze-cleaving, the selection of an appropriate nomenclature is problematical. The junctional complexes are tentatively referred to as *close junctions* (terminology after Trelstad et al., '67), pending further examination.

DISCUSSION

The differentiation of larval ascidian caudal muscle is a nearly synchronous event among cells along the entire length of the tail, but the process of differentiation does not involve the fusion of myoblasts, an event characteristic of vertebrate somatic striated muscle cells. Differentiation of the contractile apparatus immediately follows the cessation of mitosis. Cowden ('63) found no mitotic figures in presumptive muscle cells beyond the embryonic stage with a caudal bud of *Clavelina picta*, and mitosis ceases in slightly older embryos of *Perophora orientalis* (Terakado, '72) and *Distaplia occidentalis*.

The number of myoblasts in the neurulating embryo (I) of *Distaplia occidentalis* can be estimated from the mean cellular length, the average number of rows of cells in each presumptive muscle band, and the length of the caudal rudiment. Using a mean cellular length of 12.2 μ, assuming the average number of rows of cells is ten, and considering that the mean length of the caudal rudiment is 0.25 mm, there would be approximately 360 myoblasts in each presumptive muscle band. Only one additional mitotic cycle would provide the requisite number of cells for each band.

From calculations of the mean cellular volume during differentiation of the larval ascidian caudal muscle, it is known that the cells of the comma embryo (III) have significantly decreased in volume when compared with the myoblasts of either the neurulating embryo (I) or the caudate embryo (II). The decline in mean cellular volume is probably a direct result of mitosis before the synthesis of myofilaments, and all 1500 muscle cells of the two bands should be present. If the mean cellular length is 9.1 μ, the average number of rows of cells is 11, and the mean length of the embryonic tail is 0.65 mm, 1560 muscle cells are estimated to be distributed equally between the two bands. This estimation is quite comparable to the number of caudal

muscle cells, determined with serial thick Epon sections, in the swimming tadpole (VII) (Cavey and Cloney, '72).

The distribution of RNA and protein during caudal myogenesis has been studied in the simple ascidian *Clavelina picta* (Cowden, '63) and in the compound ascidian *Perophora orientalis* (Terakado, '72). RNA can be traced from the nucleus of the myoblast into a perinuclear zone before pervading the entire cytoplasm. RNA accumulates in the peripheral cytoplasm and shortly declines. The peak incorporation of ³H-uridine into RNA (or the intense cytochemical response to methyl green-pyronin) always precedes the peak incorporation of ¹⁴C-amino acids into protein (or the intense cytochemical response to alloxan-Schiff's reagent or mercuric bromphenol blue). These observations are consistent with the distribution of ribosomes and myofilaments during caudal myogenesis in embryos and larvae of *Distaplia occidentalis*. Use of the PATO reaction and techniques of differential staining permits positive identification of glycogen granules and ribosomes even though these particles overlap in size and locality. Ribosomes become increasingly abundant up to and including cells of the comma embryo (III) in which the synthesis of myofilaments begins. The level of ribosomes slowly declines in cells of the vesiculate embryo (IV) and the papillate embryo (V) while the myofibrils are growing in diameter. Ribosomes diminish until, in cells of the swimming tadpole (VII), only remnants remain (Cavey and Cloney, '72).

Myofilaments and myofibrils

Controversy over the origin of myofibrils has persisted for more than half a century. Only the classical theory that myofibrils originate from submicroscopic elements, or *Molecularfibrillen* (Heidenhain, 1899), has remained tenable.

The order of appearance of myofilaments in differentiating muscle cells is disputed. In avian skeletal muscle, several studies indicate that the thin myofilaments appear before the thick myofilaments (Allen and Pepe, '65; Obinata et al., '66; Ogawa, '62), while others argue that the thick and thin myofilaments appear simultaneously (Ferris, '59; Fischman, '67). The simultaneous appearance of both types of myofilament

is also supported by examinations of murine skeletal muscle (Bergman, '62), avian cardiac muscle (Lindner, '60), and anuran cardiac muscle (Huang, '67). The interpretation by Hay ('61) that the thick myofilaments precede the thin myofilaments in urodele skeletal muscle cells was later modified in favor of the proposition that the thick and thin myofilaments appear simultaneously (Hay, '63).

Hypotheses that suggest a temporal separation between the occurrence of the thick and thin myofilaments require careful evaluation. Failure to visualize nascent myofilaments may be attributable to their low electron densities after conventional staining of thin sections with solutions of uranium and lead. Additional enhancement (electron density) of myofilaments with a stain such as phosphotungstic acid may be required to demonstrate the presence of more than a single type of myofilament (Fischman, '67). Further, immunological assays for the first appearance of contractile proteins should be carefully examined, since the sensitivity of the assays may not be great enough to detect the initial amounts (Ogawa, '62).

The sequence of events in the differentiation of the cross-striations in myofibrils is equally confusing. In urodele skeletal muscle (Hay, '63) and avian cardiac muscle (Hibbs, '56), A-bands and I-bands evidently form before the Z-lines; the converse sequence has been inferred for avian cardiac muscle (Meyer and Queiroga, '59). In canine cardiac muscle, Schulze ('62) states that A-bands, I-bands, and Z-lines appear simultaneously, followed by the H-bands and M-lines.

Three fundamental models for the assembly of myofibrils can be envisioned (Fischman, '67):

1. *Nucleation by Z-lines*

In this model the Z-lines are constituted early in cellular differentiation. The lattice of the Z-line provides attachment sites for the thin myofilaments (Knappeis and Carlsen, '62; Reedy, '64), and the thick myofilaments associate secondarily. The correct spacing between the thick and thin myofilaments is achieved by the formation of actomyosin bridges. The model is consistent with observations on differentiating avian cardiac muscle (Wainrach and Sotelo, '61;

Weissenfels, '62) in which so-called Z-centers with attached thin myofilaments are encountered. It is also possible that Z-lines provide the sites for the assembly of myofilaments in certain skeletal muscle fibers (Hay, '63; Heuson-Stiennon, '65).

2. Primary association of thick myofilaments

In this model the thick myofilaments are initially joined by H-bridges between their naked central shafts. Thin myofilaments, either attached or unattached to Z-lines, secondarily associate with the fascicles of thick myofilaments and are correctly spaced by the formation of actomyosin bridges. There is no ultrastructural evidence of this pattern of assembly in any vertebrate striated muscle fiber.

3. Primary association of thick and thin myofilaments

In this model the thick and thin myofilaments are initially joined by actomyosin bridges. Z-lines form secondarily by interlinking the free ends of the thin myofilaments (which may already possess the protein of the Z-line). H-bridges are not implicated in the alignment of the hexagonal arrays of interdigitating thick and thin myofilaments. The model is consistent with ultrastructural observations on avian skeletal muscle (Fischman, '67). A large excess of thin myofilaments in the differentiating fiber would insure that all available sites of attachment on the thick myofilaments are saturated. There are no demonstrable H-bridges between the thick myofilaments, nor are there any aggregates consisting of only thick myofilaments. Putative material of the Z-lines always appears attached to the ends of the thin myofilaments.

In embryos of the ascidian *Perophora orientalis*, the appearance of thin myofilaments in the differentiating caudal muscle cells evidently precedes the appearance of thick myofilaments, but this interpretation is complicated by the fact that the nascent myofilaments exhibit cross-sectional diameters well below the diameters of the myofilaments in cells of the swimming tadpole. As Terakado ('72) points out, the discrepancy in cross-sectional diameters could be accounted for if the thick and thin myofilaments were derived from an heterogene-

ous population of precursors (Hay, '65). The possibility that the thick and thin myofilaments appear simultaneously cannot be conclusively dismissed. Since putative Z-lines appear after small aggregates of thick and thin myofilaments align into myofibrils, the observations are consistent with the third model for the assembly of myofibrils. The myofilaments initially join by actomyosin bridges, and the free ends of the thin myofilaments within the aggregates secondarily participate in the architecture of the Z-lines to establish the nascent myofibril.

In the ascidian *Distaplia occidentalis*, thick and thin myofilaments appear simultaneously in the peripheral sarcoplasm of cells of the comma embryo (III), and the two types of myofilament immediately associate into networks lying parallel to the sarcolemma. Myofilaments are joined by actomyosin bridges and by H-bridges. H-bridges were observed in several hundred networks of myofilaments before the full complement of thin myofilaments was present. It is inferred that the nucleus of a network is probably established through the formation of H-bridges between thick myofilaments. The larval caudal musculature of *D. occidentalis* is the only system that presently conforms to such a pattern of aggregation of myofilaments. Irrespective of which bridges form initially, the Z-lines are not essential prerequisites for the assembly.

The first networks of myofilaments in muscle cells of embryos of *Distaplia occidentalis* have no clear M-lines even though the thick myofilaments are interconnected by H-bridges. An imprecise alignment of the thin myofilaments near the center of a network may obliterate the image of the M-line when the network is viewed in longitudinal thin section.

Individual networks of myofilaments align in series, parallel to the long axis of the differentiating muscle cell, by the interposition of precursory Z-lines in the vesiculate embryo (IV). The characteristic zig-zag pattern of the Z-line is infrequently observed. Since nascent myofibrils span the entire length of the cell, growth is strictly appositional. The establishment of the primitive field of myofilaments is accompanied by feeble, sporadic contractions of the embryonic tail of living specimens in cul-

ture. An increased degree of alignment of myofilaments may result from the breakage and reformation of actomyosin bridges in the presence of tension exerted through the roughly demarcated, interconnected sarcomeres. The first contractions in cultured avian cardiac muscle also closely coincide with the appearance of Z-lines between the bundles of myofilaments (Hibbs, '56).

H-bands and M-lines in the center of the A-bands progressively appear in the papillate embryo (V) and prehatching tadpole (VI), which also display increasingly frequent contractions of the embryonic tail.

Intercalated disks and transverse myomuscular junctions

Unlike vertebrate somatic striated muscle, larval ascidian caudal muscle cells are joined by transverse myomuscular junctions. These intercellular junctional complexes superficially resemble the intercalated disks of vertebrate cardiac muscle (Berrill and Sheldon, '64; Cavey and Cloney, '72; Jackson, '58; Pucci-Minafra, '65), since both junctions are orthogonal to the primary axes of the myofibrils and both are interposed between the terminal sarcomeres of adjacent myofibrils at the level of the Z-lines. The stepped arrangement of intercalated disks and transverse myomuscular junctions are also similar. Although most transverse cellular boundaries in cardiac muscle are highly convoluted, the sarcolemmata of the caudal muscle cells of most ascidian larvae are relatively straight and produce a flattened transverse myomuscular junction (Cavey and Cloney, '72), resembling the simplified intercalated disks of the ascidian myoepithelium (Oliphant and Cloney, '72) and the atrial muscle of the turtle (Fawcett and Selby, '58).

Like the intercalated disks in vertebrate cardiac muscle (Muir, '57), the nascent myomuscular junctions between the caudal muscle cells of *Distaplia occidentalis* are often oriented obliquely rather than orthogonally to the primary axes of the myofibrils. After birth, the intercalated disks of vertebrates gradually reorient until they are situated orthogonally, and convolutions of the apposed sarcolemmata add to the complexity of the junctions. In the ascidian, the TMM junctions reorient during late embryogenesis, but the apposed sarcolem-

mata at the region of juncture never convolute.

Ascidian myomuscular junctions initially appear between the cells of the papillate embryo (V) and are situated in oblique and orthogonal orientations to the myofibrils. In the vesiculate embryo (IV), there are no morphological characteristics of the sarcolemmata or the extracellular space to indicate where a myomuscular junction will form. Unlike cultured murine cardiac muscle cells (Cedergren and Harary, '64), the apposed sarcolemmata at the TMM junction do not appear different from unapposed membranes in the immediate vicinity. The nascent myomuscular junction exhibits a constant extracellular space with a dense layer of amorphous material situated equidistant from the apposed sarcolemmal surfaces. Extracellular thin filaments, as in cultured murine cardiac muscle cells, interconnect the extracellular leaflets of apposed sarcolemmata. The extracellular space of the ascidian myomuscular junction expands until, in the prehatching tadpole (VI), it approximates the width of the space between the muscle cells of the swimming tadpole (Cavey and Cloney, '72). The extracellular dense layer disappears, leaving only the oriented filaments (cf. McNutt, '70).

The proposal by Terakado ('72) that the ascidian myomuscular junctions are responsible for the alignment of the myofibrils is not supported by any observations on the caudal muscle cells of *Distaplia occidentalis*. The differentiation of the myomuscular junctions always follows the establishment of the nascent field of myofilaments in the peripheral sarcoplasm.

Sarcoplasmic reticulum, transverse tubules, and peripheral couplings

In the vast majority of skeletal and cardiac muscle fibers studied, there are two separate systems of membranes: a system of transverse tubules (T-tubules) and the sarcoplasmic reticulum (Andersson-Cedergren, '59; Bennett and Porter, '53; Porter, '61; Porter and Palade, '57). Each transverse tubule is an invagination of the sarcolemma. Markers such as ferritin (Huxley, '64; Page, '64), albumin (Hill, '64), and certain fluorescent dyes (Endo, '66) penetrate the lumen of the T-tubule and conclusively demonstrate that it is an extra-

cellular compartment. Such experiments are in accord with ultrastructural observations (Franzini-Armstrong and Porter, '64; Walker and Schrodt, '65). The T-tubular system is oriented orthogonally to the primary axes of the myofibrils in muscle fibers of adult organisms, and the T-tubules are interconnected by longitudinal tubules (Revel, '62).

The sarcoplasmic reticulum is a network of tubules investing the myofibrils. Two cisternae of SR from adjacent sarcomeres are commonly apposed to a single T-tubule, forming a *triad* (Porter and Palade, '57). The cisterna of SR and the T-tubule are separated by a gap that is approximately 100 Å wide (Andersson-Cedergren, '59; Revel, '62; Walker and Schrodt, '66), and periodic dense structures traverse the gap (Franzini-Armstrong, '64; Revel, '62) and may physically join the two systems of membranes (Walker and Schrodt, '66). A physical connection between the SR and the T-tubule could couple the events of excitation of the cellular membrane and contraction of the myofibrils, since disruption of the T-tubules inhibits contraction but does not interfere with the depolarization of the cellular membrane (Gage and Eisenberg, '67).

In fetal (Walker and Schrodt, '68) and newborn (Schiaffino and Margreth, '69) murine skeletal muscle, cisternae of the SR form an irregular network about the myofibrils that is continuous between sarcomeres but bears no patterned association with the bands the sarcomere. Smooth-surfaced reticular membranes may originate as projections from rough-surfaced endoplasmic reticulum when eventually fuse into a network (Ezerman and Ishikawa, '67; Schiaffino and Margreth, '69). The rough-surfaced endoplasmic reticulum, in turn, probably derives from evaginations of the nuclear envelope (Walker and Edge, '71). T-tubules form as inpocketings of the sarcolemma, and they proliferate by branching and budding (Ezerman and Ishikawa, '67). The first T-tubules appear only in the peripheral sarcoplasm and gradually penetrate the endoplasm as differentiation proceeds. Very few triads are observed in fetal (Walker and Schrodt, '68) or newborn (Schiaffino and Margreth, '69) murine skeletal muscle, and those triads that do occur are usually aligned in parallel with

the myofibrils (instead of orthogonally to them). The initial gap between a cisterna of SR and a T-tubule is on the order of 100–200 Å, and the periodic densities within it form later (Ezerman and Ishikawa, '67). As differentiation proceeds, the triads proliferate and assume orientations orthogonal to the primary axes of the myofibrils (Edge, '70; Luff and Atwood, '71).

In certain cardiac muscle cells of mammals (Fawcett and McNutt, '69; Johnson and Sommer, '67; McNutt and Fawcett, '69; Sommer and Johnson, '68), in cardiac muscle cells of birds (Jewett et al., '71, '73), and in the cardiac muscle cells of amphibians (Gros and Schrével, '70; Sommer and Johnson, '68), a T-tubular system is absent. Instead, cisternae of sarcoplasmic reticulum (subsarcolemmal cisternae) are found in close apposition with a non-invaginated sarcolemma. Such peripheral couplings between the SR and sarcolemma are also described in the ascidian myocardium (Oliphant and Cloney, '72) and in the larval ascidian caudal muscle cells (Cavey and Cloney, '72).

Morphologically, peripheral couplings resemble the diadic connections established between the sarcoplasmic reticulum and sarcolemma or nascent T-tubule in developing mammalian skeletal muscle cells (Kelly, '69, '71; Schiaffino and Margreth, '69). Subsarcolemmal cisternae of peripheral couplings in larval ascidian caudal muscle cells (Cavey and Cloney, '72) exhibit the intracisternal coextensive densities common to apposed cisternae of SR in vertebrate skeletal and cardiac muscles (Edge, '70; Walker and Schrodt, '65). Presumably, the proximity of myofibrils to the sarcolemma facilitates a direct contact with the sarcoplasmic reticulum over relatively short distances (a few microns) so that T-tubules become unnecessary.

With the exception of the present study, there are no data on the formation of peripheral couplings in a muscle fiber without a T-tubular system as well. In the ascidians *Ciona intestinalis* (Pucci-Minafra, '65) and *Perophora orientalis* (Terakado, '72), vesicular structures are observed between the myofibrils of the caudal muscle cells. Such vesicles may be the remnants of the sarcoplasmic reticulum following fixation of the tissue by osmium alone. In the swimming tadpole (VII) of *Distaplia*

occidentalis, fixation of the muscle cells with glutaraldehyde and osmium reveals an elaborate system of SR in the field of myofibrils and numerous peripheral couplings on all surfaces of the sarcolemma. It is conclusively demonstrated that fixation by osmium alone destroys the organization of the sarcoplasmic reticulum (Cavey and Cloney, '72).

The accumulated evidence from differentiating caudal muscle cells of *Distaplia occidentalis* indicates that the "interdigitating" model of the transverse collar of SR encircling the H-band is correct (Cavey and Cloney, '72). The collar begins to form in cells of the papillate embryo (V), when the transverse collar of SR overlying the I-band is already fully formed. In the prehatching tadpole (VI), the H-band is invested by a single perforated sheet of SR that is discontinuous at the side of the myofibril most distant from the sarcolemma. The free ends of the sheet are visualized at the raphe, and the absence of peripheral couplings near the H-band is suggestive that the sheet elevates from the surface of the myofibril, recurves (thus forming the characteristic double layer), and extends peripherally to participate in peripheral couplings. Extensive interdigitations at the raphe near the zone of recurvation and between the two intimately apposed layers would produce the complex architecture of the collar observed in functional muscle cells of the swimming tadpole (VII).

The initial source of reticular membranes in ascidian caudal muscle cells is probably the nuclear envelope. Evaginations produce ribosome-studded reticular membranes in the myoblasts of the neurulating embryo (I) and the caudate embryo (II). Rough-surfaced ER is similarly constituted in murine skeletal muscle cells (Walker and Edge, '71). In the feline myocardium, evaginations of the nuclear envelope may contribute membranes to the active Golgi body (Fawcett and McNutt, '69). Through the gradual loss of bound ribosomes, rough-surfaced SR becomes smooth-surfaced SR within the caudal muscle cells of the ascidian. In differentiating (Ezerman and Ishikawa, '67; Luff and Atwood, '71; Walker and Edge, '71) and denervated (Margreth et al., '66; Muscatello et al., '65) skeletal muscle cells, it is frequently noted that rough-surfaced SR transforms into smooth-

surfaced SR or that the decline in rough-surfaced SR is paralleled by an increase in smooth-surfaced SR (Dessouky and Hibbs, '65). The homology between rough- and smooth-surfaced reticular membranes is also evident in tissues other than muscle (Dallner et al., '66; Jones and Fawcett, '66).

The elaborate configuration of the sarcoplasmic reticulum about the myofibrils in ascidian caudal muscle cells is established much later than the field of myofibrils. The SR bears no relationship to the nascent myofibrils in cells of the vesiculate embryo (IV), although the membranes of the sarcoplasmic reticulum are proliferating. This is not characteristic of certain vertebrate skeletal muscle cells. Dessouky and Hibbs ('65) note that smooth-surfaced vesicles envelop the myofibrils of avian skeletal muscle cells quite early during differentiation, and Walker and Edge ('71) have shown that the SR in murine skeletal muscle cells forms even before the Z-lines, possibly indicating that the SR assists in the formation of them since filamentous strands seemingly connect the cisternae of SR and the differentiating Z-lines.

The gaps between the sarcoplasmic reticulum and the sarcolemma (or T-tubule) are variously structured. Periodic densities in the gaps are described in a number of studies on vertebrate skeletal (Peachey, '65; Revel, '62) and cardiac (Gros and Schrével, '70; Jewett et al., '71) muscles. It is postulated that the periodic densities are areas of focal tight junctions between the cellular membrane and the sarcoplasmic reticulum (Franzini-Armstrong, '70; Kelly, '67; Kelly and Cahill, '69). Periodic densities are not observed in the gaps of the peripheral couplings in the feline myocardium (Fawcett and McNutt, '69), in the ascidian myoepithelium (Oliphant and Cloney, '72), or in the caudal muscle cells of the ascidian larva (Cavey and Cloney, '72). Instead, a dense plaque, with or without a periodicity, is situated equidistant from both apposed membranes.

In the comma embryo (III) of the ascidian, the appearance of peripheral couplings coincides with the appearance of the first myofibrils. In the initial apposition of the two membranes of a coupling, the central plaque in the junctional gap and the coextensive densities in the subsarcolemmal cisterna are absent. Membranous co-

extensive densities in the apposed cisterna of SR appear only after apposition with the sarcolemma or T-tubule in differentiating murine skeletal muscle (Edge, '70) and only in the functional caudal muscle cells of the ascidian swimming tadpole (VII) (Cavey and Cloney, '72).

It has been suggested that the formation of peripheral couplings is an intermediate stage in the formation of the transverse tubular system. The first associations between the SR and the sarcolemma in murine skeletal muscle cells are couplings at the cellular periphery (Schiaffino and Margreth, '69). It is plausible that the peripheral couplings become interiorized by caveolation of the sarcolemma and thus constitute a T-tubular system (Kelly, '71).

A few ultrastructural studies on vertebrate skeletal muscle include estimates of the relative cellular volume occupied by cisternae of the sarcoplasmic reticulum. The SR occupies approximately four to five per cent of the volume of the sartorius muscle fiber of the frog (Peachey, '65) and five and one-half per cent of the volume of the soleus muscle fiber of the mouse (Luff and Atwood, '71). In the swimming tadpole (VII) of *Distaplia occidentalis*, the present study has determined that slightly more than four per cent of the volume of the caudal muscle cell is constituted of sarcoplasmic reticulum.

The caudal muscle cells of the swimming tadpoles of most simple and compound ascidians contain a single row of cortical myofibrils. Peripheral couplings meet the requirement for a specific association between the sarcoplasmic reticulum and the sarcolemma. In the didemnid aplousobranch ascidian *Diplosoma macdonaldi*, however, the myofibrils are situated near the endoplasm of the muscle cell. It would be predicted that a system of transverse tubules is required for excitation-contraction coupling. The lack of peripheral couplings is substantiated ultrastructurally, but other obvious dissimilarities to vertebrate somatic striated muscle exist (M. J. Cavey and R. A. Cloney, unpublished observations).

Other cellular organelles

Terakado ('72) has documented the change in the nuclear and nucleolar morphologies and the correlations between

nucleolar activity, concentration of ribosomes, and synthesis of protein in differentiating larval ascidian caudal muscle cells of *Perophora orientalis*, both cytochemically and ultrastructurally. Comparable correlations, made from calculations of the relative cellular volume occupied by the major classes of organelles, apply to embryos and larvae of *Distaplia occidentalis*.

Annulate lamellae commonly occur in the nuclei of myoblasts of the neurulating embryo (I) and the caudate embryo (II). The significance is unknown, however abundant intranuclear systems of membranes have been described in developing ascidian oocytes and probably originate from detached evaginations of the nuclear envelope (Kessel, '65).

Large stores of glycogen in the functional muscle cells of the swimming tadpole (VII) are a potential energy source for the contractions of the myofibrils. Glycogen presumably originates through the degradation of the proteid-yolk granules in the presumptive and definitive caudal muscle cells. It is postulated that the fusion of a putative primary lysosomal granule and a proteid-yolk granule is the initial stage in the conversion of yolk to glycogen. Glycogen granules appear to radiate from the peripheries of the degrading yolk granules. Activity of the Golgi apparatus immediately precedes the period of intensive degradation of yolk, suggesting that the Golgi apparatus may be packaging some of the enzymes for glycogenesis (in the PPL granules). If glycogenesis truly relies on the fusion of primary lysosomes and yolk granules, tests for hydrolytic enzymes should determine if the logical temporal characteristics are followed. It would be expected that the hydrolytic enzymes are (1) packaged by the Golgi apparatus, (2) contained by the putative primary lysosomal granules, and (3) combined with the large storage granules of yolk. Correlations presented in this report, exist between the decline in proteid-yolk and the rise in the cellular content of glycogen granules, between the onset of degradation of proteid-yolk and the content of putative primary lysosomes, and between the activity of the Golgi apparatus and the content of putative primary lysosomes. Since the proteid-yolk granules and the PPL granules are often morphologically indistinguishable

except in terms of size, the working hypothesis of Bluemink ('69) that functional lysosomes in cells of the pulmonate snail *Limnaea stagnalis* are similar to yolk granules must be carefully considered. The findings on this aspect of caudal myogenesis in embryos and larvae of *Distaplia occidentalis* will be examined in the third and final report on this species.

In definitive caudal muscle cells which have lost most of their yolk reserves, the level of PPL granules remains relatively high, possibly indicating that they participate in processes other than glycogenesis and/or the destruction of old or defective organelles. Upon resorption of the axial complex at metamorphosis, the caudal muscle cells are pushed into the posterior cavity in the trunk of the larva (Cloney, '66) and phagocytized (R. A. Cloney, unpublished observations). Mobilization of the stored glycogen in the caudal muscle cells may contribute to the energy pool for post-metamorphic differentiation. The caudal muscle cells could begin autodigestion owing to their constitutive PPL granules. During postnatal differentiation of murine skeletal muscle, the glycogen accumulated by the foetus is degraded by autolysosomes. Smooth-surfaced vesicles, derived from the Golgi body, enclose areas of the cytoplasm and digest the glycogen granules. Acid phosphatase activity is detected in the Golgi apparatus and in the cisternae of the endoplasmic reticulum (Schiaffino and Hanzlíková, '72). Postnatal mobilization of glycogen for continued cellular differentiation is common among many mammalian skeletal muscles (Jézéquel et al., '65).

Sarcolemmata and close junctions

Between dividing myoblasts of the neuroectodermal embryo (I) and the caudate embryo (II), junctional complexes with exceptionally wide (250 Å) extracellular spaces are formed. The close junctions between caudal muscle cells of the swimming tadpole (VII) have an extracellular gap that is only 30–40 Å wide (Cavey and Cloney, '72). Junctional complexes with the wide extracellular spaces may be nascent close junctions in the process of differentiation, or they may be labile cellular contacts which provide a temporary attachment. The primordial cells of the anuran heart similarly produce filopodia that are joined by a small number of tight (probably close) junctions

(Huang, '67). Close junctions with relatively wide extracellular spaces also join differentiating murine skeletal muscle cells (Kelly and Zacks, '69).

In the ascidian, close junctions form between sarcolemmata in a manner similar to the mode of formation of the transverse myomuscular junctions, the only other specialized contacts between the caudal muscle cells. Apposed sarcolemmata become parallel to each other, and fibrous material appears in the intervening extracellular space. A dense matrix, equidistant from either sarcolemma, is laid down and extracellular filaments interconnect the two outer leaflets of the membranes across the junctional space. Unlike the process resulting in formation of a transverse myomuscular junction, the extracellular junctional space is almost completely eliminated in the formation of a close junction.

ACKNOWLEDGMENTS

A large part of this investigation was carried out at the Friday Harbor Laboratories of the University of Washington. The cooperation and helpful suggestions of the Director, Dr. Robert L. Fernald, are gratefully acknowledged.

Dr. John H. Luft of the Department of Biological Structure, University of Washington, generously supplied unpublished protocols for the use of ruthenium red in fixation and for the removal of epoxy resins from sectioned tissues. Dr. John M. Palka of the Department of Zoology provided use of his desk computer which enormously speeded the repetitious mathematical computations.

LITERATURE CITED

- Allen, E. R., and F. A. Pepe 1965 Ultrastructure of developing muscle cells in the chick embryo. *Am. J. Anat.*, 116: 115–148.
- Andersson-Cedergren, E. 1959 Ultrastructure of motor end plate and sarcoplasmic components of mouse skeletal muscle fiber as revealed by three-dimensional reconstructions from serial sections. *J. Ultrastruct. Res.*, 1 (Suppl.): 1–191.
- Bancroft, F. W. 1899 Oogenesis in *Distaplia occidentalis* Ritter (MS.), with remarks on other species. *Bull. Mus. Comp. Zool. Harvard*, 35: 59–112.
- Bennett, H. S., and K. R. Porter 1953 An electron microscope study of sectioned breast muscle of the domestic fowl. *Am. J. Anat.*, 93: 61–105.
- Bergman, R. A. 1962 Observations on the morphogenesis of rat skeletal muscle. *Bull. Johns Hopkins Hosp.*, 110: 187–201.
- Berrill, N. J., and H. Sheldon 1964 The fine structure of the connections between muscle cells in

- ascidian tadpole larva. *J. Cell Biol.*, 23: 664-669.
- Bluemink, J. G. 1969 Are yolk granules related to lysosomes? *Zeiss Information*, 73: 95-99.
- Cavey, M. J., and R. A. Cloney 1972 Fine structure and differentiation of ascidian muscle. I. Differentiated caudal musculature of *Distaplia occidentalis* tadpoles. *J. Morph.*, 138: 349-374.
- Cedergren, B., and I. Harary 1964 *In vitro* studies on single beating rat heart cells. VII. Ultrastructure of the beating cell layer. *J. Ultrastruct. Res.*, 11: 443-454.
- Cloney, R. A. 1964 Development of the ascidian notochord. *Acta Embryol. Morphol. Exper.*, 7: 111-130.
- 1966 Cytoplasmic filaments and cell movements: Epidermal cells during ascidian metamorphosis. *J. Ultrastruct. Res.*, 14: 300-328.
- 1972 Cytoplasmic filaments and morphogenesis: Effects of cytochalasin B on contractile epidermal cells. *Z. Zellforsch.*, 132: 167-192.
- Cowden, R. R. 1963 RNA and protein distribution during the development of axial mesodermal structures in the ascidian, *Clavelina picta*. Wilhelm Roux' Arch. Entwickl.-Mech. Org., 154: 526-532.
- Dallner, G., P. Siekevitz and G. E. Palade 1966 Biogenesis of endoplasmic reticulum membranes. I. Structural and chemical differentiation in developing rat hepatocyte. *J. Cell Biol.*, 30: 73-96.
- Dessouky, D. A., and R. G. Hibbs 1965 An electron microscope study of the development of the somatic muscle of the chick embryo. *Am. J. Anat.*, 116: 523-566.
- Edge, M. B. 1970 Development of apposed sarcoplasmic reticulum at the T system and sarcolemma and the change in orientation of triads in rat skeletal muscle. *Dev. Biol.*, 23: 634-650.
- Endo, M. 1966 Entry of fluorescent dyes into the sarcotubular system of the frog muscle. *J. Physiol.*, 185: 224-238.
- Ezerman, E. B., and H. Ishikawa 1967 Differentiation of the sarcoplasmic reticulum and T system in developing chick skeletal muscle *in vitro*. *J. Cell Biol.*, 35: 405-420.
- Fawcett, D. W., and N. S. McNutt 1969 The ultrastructure of the cat myocardium. I. Ventricular papillary muscle. *J. Cell Biol.*, 42: 1-45.
- Fawcett, D. W., and C. C. Selby 1958 Observations on the fine structure of the turtle atrium. *J. Biophys. Biochem. Cytol.*, 4: 63-72.
- Ferris, W. 1959 Electron microscope observations of the histogenesis of striated muscle. *Anat. Rec.*, 133: 275.
- Fischman, D. A. 1967 An electron microscope study of myofibril formation in embryonic chick skeletal muscle. *J. Cell Biol.*, 32: 557-575.
- Franzini-Armstrong, C. 1964 Fine structure of sarcoplasmic reticulum and transverse tubular system in muscle fibers. *Fed. Proc., Fed. Amer. Soc. Exp. Biol.*, 23: 887-895.
- 1970 Studies of the triad. I. Structure of the junction in frog twitch fibers. *J. Cell Biol.*, 47: 488-499.
- Franzini-Armstrong, C., and K. R. Porter 1964 Sarcolemmal invaginations constituting the T system in fish muscle fibers. *J. Cell Biol.*, 22: 675-696.
- Gage, P. W., and R. S. Eisenberg 1967 Action potentials without contraction in frog skeletal muscle fibers with disrupted transverse tubules. *Science*, 158: 1702-1703.
- Gros, D., and J. Schrével 1970 Ultrastructure comparée du muscle cardiaque ventriculaire de l'ambystome et de sa larve, l'axolotl. *J. Microscopie*, 9: 765-784.
- Hay, E. D. 1961 Fine structure of differentiating muscle in developing myotomes of *Amblystoma opacum* larvae. *Anat. Rec.*, 139: 236.
- 1963 The fine structure of differentiating muscle in the salamander tail. *Z. Zellforsch.*, 59: 6-34.
- 1965 Metabolic patterns in limb development and regeneration. In: *Organogenesis*. R. L. DeHaan and H. Ursprung, eds. Holt, Rinehart and Winston, Inc., New York, pp. 315-336.
- Heidenhain, M. 1899 Beiträge zur Aufklärung des wahren Wesens der faserförmigen Differenzierungen. *Anat. Anz.*, 16: 97-131.
- Heuson-Stiennon, J.-A. 1965 Morphogenèse de la cellule musculaire striée, étudiée au microscope électronique. I. Formation des structures fibrillaires. *J. Microscopie*, 4: 657-678.
- Hibbs, R. G. 1956 Electron microscopy of developing cardiac muscle in chick embryos. *Am. J. Anat.*, 99: 17-51.
- Hill, D. K. 1964 The space accessible to albumin within the striated muscle fibre of the toad. *J. Physiol.*, 175: 275-294.
- Huang, C. Y. 1967 Electron microscopic study of the development of heart muscle of the frog *Rana pipiens*. *J. Ultrastruct. Res.*, 20: 211-226.
- Huxley, H. E. 1964 Evidence for continuity between the central elements of the triads and extracellular space in frog sartorius muscle. *Nature*, 202: 1067-1071.
- Jackson, S. F. 1958 Some aspects of morphogenesis in ascidians. *Biol. Bull.*, 115: 335.
- Jewett, P. H., S. D. Leonard and J. R. Sommer 1973 Chicken cardiac muscle. Its elusive extended junctional sarcoplasmic reticulum and sarcoplasmic reticulum fenestrations. *J. Cell Biol.*, 56: 595-600.
- Jewett, P. H., J. R. Sommer and E. A. Johnson 1971 Cardiac muscle. Its ultrastructure in the finch and hummingbird with special reference to the sarcoplasmic reticulum. *J. Cell Biol.*, 49: 50-65.
- Jézéquel, A.-M., K. Arakawa and J. W. Steiner 1965 The fine structure of the normal, neonatal mouse liver. *Lab. Invest.*, 14: 1894-1930.
- Johnson, E. A., and J. R. Sommer 1967 A strand of cardiac muscle. Its ultrastructure and the electrophysiological implications of its geometry. *J. Cell Biol.*, 33: 103-129.
- Jones, A. L., and D. W. Fawcett 1966 Hypertrophy of the agranular endoplasmic reticulum in hamster liver induced by phenobarbital (with a review on the functions of this organelle in liver). *J. Histochem. Cytochem.*, 14: 215-232.
- Kelly, A. M. 1969 Sarcoplasmic reticulum and the transverse tubular system in developing rat intercostal muscle. *J. Cell Biol.*, 43: 65a-66a.
- 1971 Sarcoplasmic reticulum and T tubules in differentiating rat skeletal muscle. *J. Cell Biol.*, 49: 335-344.
- Kelly, A. M., and S. I. Zacks 1969 The histogenesis of rat intercostal muscle. *J. Cell Biol.*, 42: 135-153.
- Kelly, D. E. 1967 Fine structural analysis of muscle triad junctions. *J. Cell Biol.*, 35: 66A.

- Kelly, D. E., and M. A. Cahill 1969 Skeletal muscle triad junction fine structure; new observations regarding dimples of the sarcoplasmic reticulum terminal cisternae. *J. Cell Biol.*, 43: 66a.
- Kessel, R. G. 1965 Intracellular and cytoplasmic annulate lamellae in tunicate oocytes. *J. Cell Biol.*, 24: 471-487.
- Knappeis, G. G., and F. Carlsen 1962 The ultrastructure of the Z disc in skeletal muscle. *J. Cell Biol.*, 13: 323-335.
- Lindner, E. 1960 Myofibrils in the early development of chick embryo hearts as observed with the electron microscope. *Anat. Rec.*, 136: 234-235.
- Luff, A. R., and H. L. Atwood 1971 Changes in the sarcoplasmic reticulum and transverse tubular system of fast and slow skeletal muscles of the mouse during postnatal development. *J. Cell Biol.*, 51: 369-383.
- Luft, J. H. 1961 Improvements in epoxy resin embedding methods. *J. Biophys. Biochem. Cytol.*, 9: 409-414.
- Margreth, A., F. Novello and M. Aloisi 1966 Unbalanced synthesis of contractile and sarcoplasmic proteins in denervated frog muscle. *Exptl. Cell Res.*, 41: 666-706.
- McNutt, N. S. 1970 Ultrastructure of intercellular junctions in adult and developing cardiac muscle. *Am. J. Cardiol.*, 25: 169-183.
- McNutt, N. S., and D. W. Fawcett 1969 The ultrastructure of the cat myocardium. II. Atrial muscle. *Am. J. Cardiol.*, 25: 169-183.
- Meyer, H., and L. T. Queiroga 1959 An electron microscope study of embryonic heart muscle cells grown in tissue cultures. *J. Biophys. Biochem. Cytol.*, 5: 169-170.
- Muir, A. R. 1957 An electron microscope study of the embryology of the intercalated disc in the heart of the rabbit. *J. Biophys. Biochem. Cytol.*, 3: 193-202.
- Muscattello, U., A. Margreth and M. Aloisi 1965 On the differential response of sarcoplasm and myoplasm to denervation in frog muscle. *J. Cell Biol.*, 27: 1-24.
- Obinata, T., M. Yamamoto and K. Maruyama 1966 The identification of randomly formed thin filaments in differentiating muscle cells of the chick embryo. *Dev. Biol.*, 14: 192-213.
- Ogawa, Y. 1962 Synthesis of skeletal muscle proteins in early embryos and regenerating tissue of chick and *Triturus*. *Exptl. Cell Res.*, 26: 269-274.
- Oliphant, L. W., and R. A. Cloney 1972 The ascidian myocardium: Sarcoplasmic reticulum and excitation-contraction coupling. *Z. Zellforsch.*, 129: 395-412.
- Page, S. G. 1964 The organization of the sarcoplasmic reticulum in frog muscle. *J. Physiol.*, 175: 10P-11P.
- Peachey, L. D. 1965 The sarcoplasmic reticulum and transverse tubules of the frog's sartorius. *J. Cell Biol.*, 25: 209-231.
- Porter, K. R. 1961 The sarcoplasmic reticulum. Its recent history and present status. *J. Biophys. Biochem. Cytol.*, 10 (Suppl.): 219-226.
- Porter, K. R., and G. E. Palade 1957 Studies on the endoplasmic reticulum. III. Its form and distribution in striated muscle cells. *J. Biophys. Biochem. Cytol.*, 3: 269-300.
- Pucci-Minafra, I. 1965 Ultrastructure of muscle cells in *Ciona intestinalis* tadpoles. *Acta Embryol. Morphol. Exper.*, 8: 289-305.
- Reedy, M. K. 1964 Remarks at a discussion on the physical and chemical basis of muscular contraction. *Proc. Roy. Soc. London*, 160B: 458-460.
- Revel, J. P. 1962 The sarcoplasmic reticulum of the bat cricothyroid muscle. *J. Cell Biol.*, 12: 571-588.
- Revel, J. P., L. Napolitano and D. W. Fawcett 1960 Identification of glycogen in electron micrographs of thin tissue sections. *J. Biophys. Biochem. Cytol.*, 8: 575-589.
- Reynolds, E. S. 1963 The use of lead citrate at high pH as an electron-opaque stain in electron microscopy. *J. Cell Biol.*, 17: 208-212.
- Richardson, K. C., L. Jarett and E. H. Finke 1960 Embedding in epoxy resins for ultrathin sectioning in electron microscopy. *Stain Technol.*, 35: 313-323.
- Schiaffino, S., and V. Hanzlíková 1972 Autophagic degradation of glycogen in skeletal muscles of the newborn rat. *J. Cell Biol.*, 52: 41-51.
- Schiaffino, S., and A. Margreth 1969 Coordinated development of the sarcoplasmic reticulum and T system during postnatal differentiation of rat skeletal muscle. *J. Cell Biol.*, 41: 855-875.
- Schulze, W. 1962 Elektronenmikroskopische Untersuchung des embryonalen Hundeherzmuskels. *Z. Mikr.-Anat. Forsch.*, 68: 271-284.
- Sommer, J. R., and E. A. Johnson 1968 Cardiac muscle. A comparative study of Purkinje fibers and ventricular fibers. *J. Cell Biol.*, 36: 497-526.
- Terakado, K. 1972 Cytological and ultrastructural studies on muscle differentiation in the ascidian, *Perophora orientalis*. Development, Growth and Differentiation, 14: 1-23.
- Trelstad, R. L., E. D. Hay and J. P. Revel 1967 Cell contact during early morphogenesis in the chick embryo. *Dev. Biol.*, 16: 78-106.
- Vye, M. V., and D. A. Fischman 1971 A comparative study of three methods for the ultrastructural demonstration of glycogen in thin sections. *J. Cell Sci.*, 9: 727-749.
- Wainrach, S., and J. R. Sotelo 1961 Electron microscope study of the developing chick embryo heart. *Z. Zellforsch.*, 55: 622-634.
- Walker, S. M., and M. B. Edge 1971 The sarcoplasmic reticulum and development of Z lines in skeletal muscle fibers of fetal and postnatal rats. *Anat. Rec.*, 169: 661-678.
- Walker, S. M., and G. R. Schrodt 1965 Continuity of the T system with the sarcolemma in rat skeletal muscle fibers. *J. Cell Biol.*, 27: 671-677.
- 1966 Connections between the T system and sarcoplasmic reticulum. *Anat. Rec.*, 155: 1-10.
- 1968 Triads in skeletal muscle fibers of 19-day fetal rats. *J. Cell Biol.*, 37: 564-569.
- Weissenfels, N. 1962 Der Einfluss der Gewebezüchtung auf die Morphologie der Hühnerherzmuskelzellen. IV. Über Differenzierungs- und Abbauvorgänge an den Muskelelementen. *Protoplasma (Wien)*, 55: 99-113.
- Wood, R. L., and J. H. Luft 1965 The influence of buffer systems on fixation with osmium tetroxide. *J. Ultrastruct. Res.*, 12: 22-45.

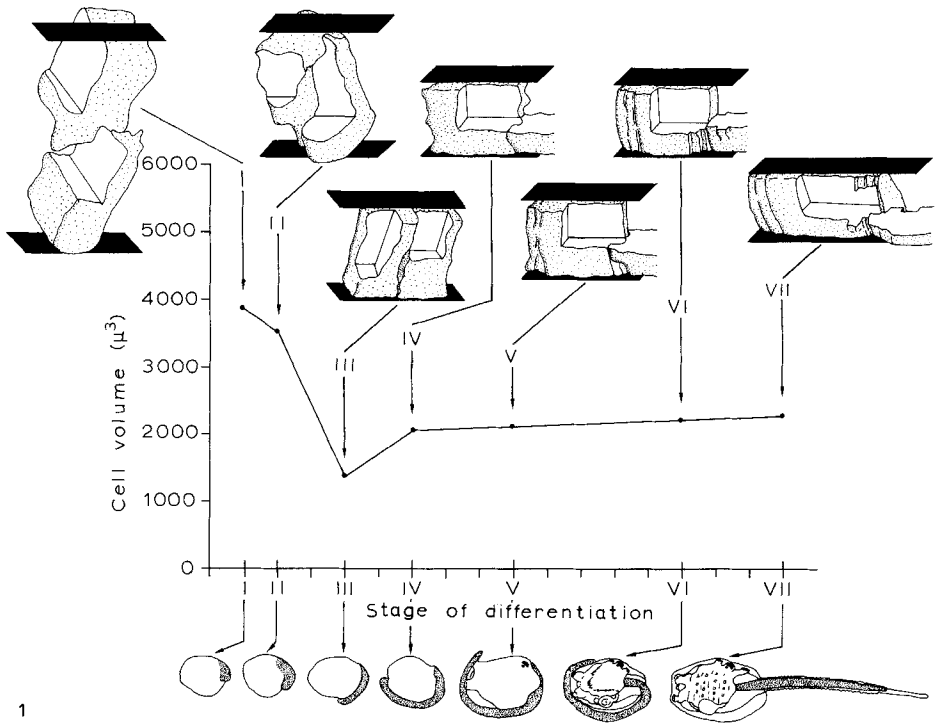
Abbreviations for Plates

A, sarcomeric A-band	Ly, putative primary lysosomal granule
AnL, annulate lamella	mb, muscle band
bb, branchial basket	Mf, myofibril or field of myofilaments
BL, basal lamina	Mfl, myofilament or network of myofilaments
c, cavity of larval trunk	MIB, multilamellar body
cb, caudal bud	Mt, mitochondrion
CJ, close junction	ng, neural groove
cr, caudal rudiment	Nl, nucleolus
EL, external lamina	no, notochord
Ep, epidermis	np, pore in nuclear envelope
es, excurrent siphon	Nu, nucleus
Gly, glycogen granules/rosettes	p, adhesive papilla
Go, Golgi apparatus	PC, peripheral coupling
H, sarcomeric H-band	Pl, plasmalemma of presumptive muscle cell
HSR, sarcoplasmic reticulum centered on M-line and encircling H-band	r, ribosome or polysome
I, sarcomeric I-band	RER, rough-surfaced endoplasmic reticulum
Id, cellular interdigitation	RSR, rough-surfaced sarcoplasmic reticulum
is, incurrent siphon	Sl, sarcolemma of definitive muscle cell
ISR, sarcoplasmic reticulum centered on Z-line and encircling I-band	SR, smooth-surfaced sarcoplasmic reticulum
JC, junctional complex between plasmalemmata	SSC, subsarcolemmal cisterna
LDA, area of low electron density of transverse myomuscular junction	sv, sensory vesicle
	Yo, proteid-yolk granule
	Z, sarcomeric Z-line
	Zm, Z-matrix

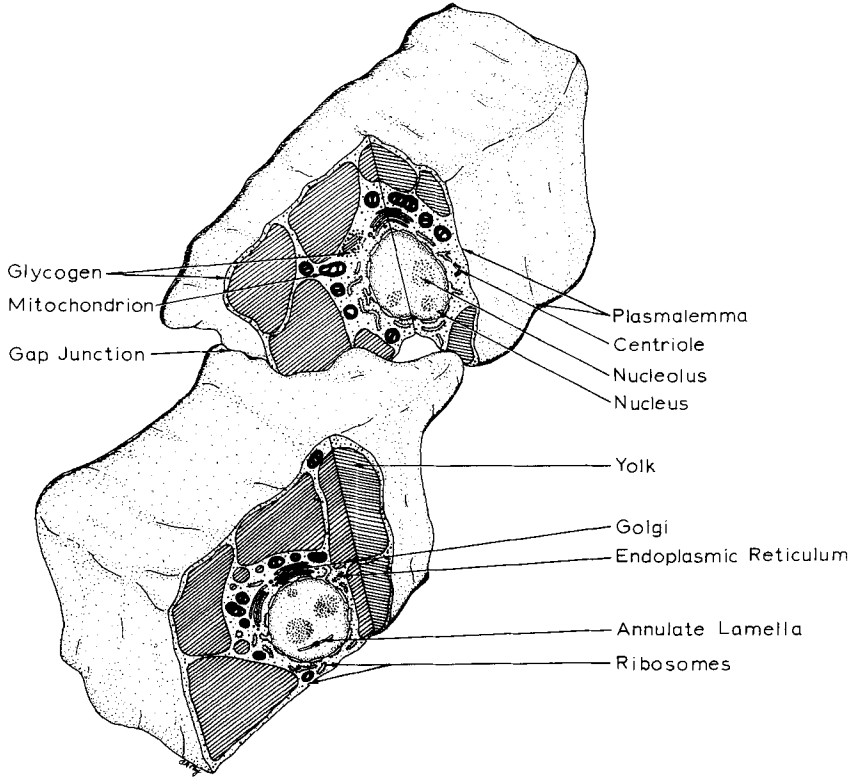
PLATE I

EXPLANATION OF FIGURES

- 1 Change in mean volume of caudal muscle cells of *Distaplia occidentalis* during embryogenesis. Roman numerals designate the seven stages of cellular differentiation used in this study and the appropriate embryo or larva beneath the abscissa (I, neurulating embryo; II, caudate embryo; III, comma embryo; IV, vesiculate embryo; V, papillate embryo; VI, prehatching tadpole; VII, swimming tadpole). The spacings between the designated stages of caudal myogenesis are proportional to time (table 1), and the depicted embryos and larvae are drawn to the same scale. Cellular shape and orientation relative to the epidermal and notochordal boundaries (planes above and below insets) of the presumptive or definitive muscle band are shown above the plotted data points. Insets depicting the differentiating cells are drawn to the same scale, and these diagrams are reproduced with additional detail in figures 2-7.
- 2 Schematic diagram of cells in the presumptive muscle bands of the caudal rudiment of the neurulating embryo (stage I of caudal myogenesis). The depicted cells are comparable to cells situated in all parts of a presumptive muscle band (table 2). The orientation of the cells in relation to the epidermis and the notochord is indicated in figure 1. The shape of the cells and the distribution of organelles in this drawing and in figures 3-7 are typical, but certain ultrastructural features are simplified for clarity.



1



2

PLATE 2

EXPLANATION OF FIGURES

- 3 Schematic diagram of cells in the presumptive muscle bands of the caudate embryo (stage II of caudal myogenesis). The illustrated cells are typical of those found in all parts of a presumptive muscle band (table 2). The long axis of the cell is perpendicular to the long axis of the muscle band (fig. 1).
- 4 Schematic diagram of cells in the muscle bands of the comma embryo (stage III of caudal myogenesis). The shape of each cell is dependent on its position within the muscle band (table 2); the depicted cells are representative of those situated in the dorsal and ventral parts of the band. The long axis of the cell is perpendicular to the long axis of the muscle band (fig. 1).

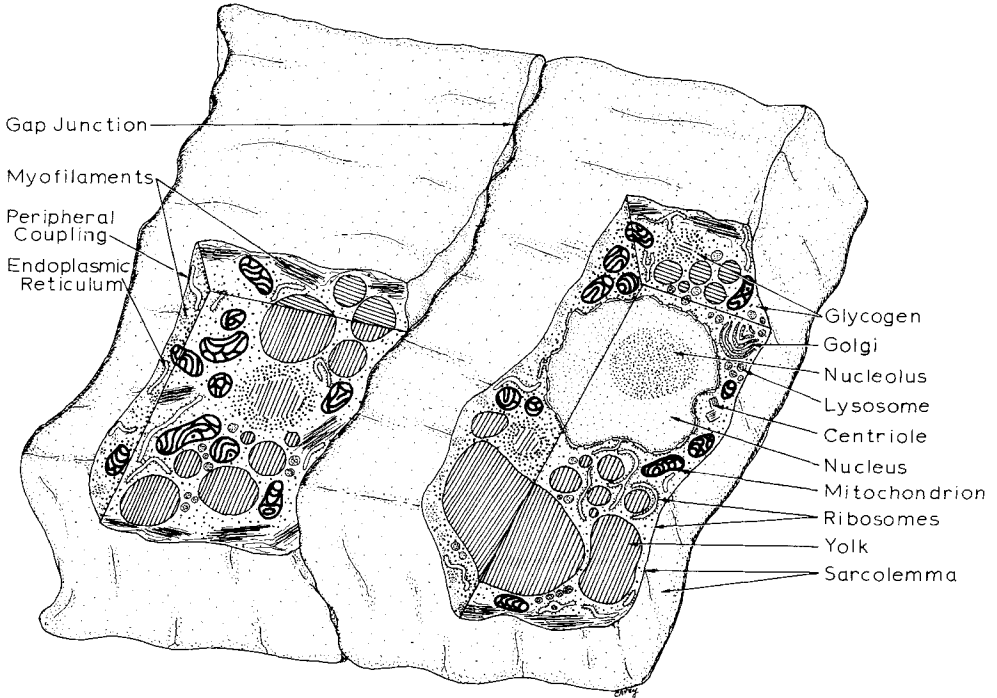
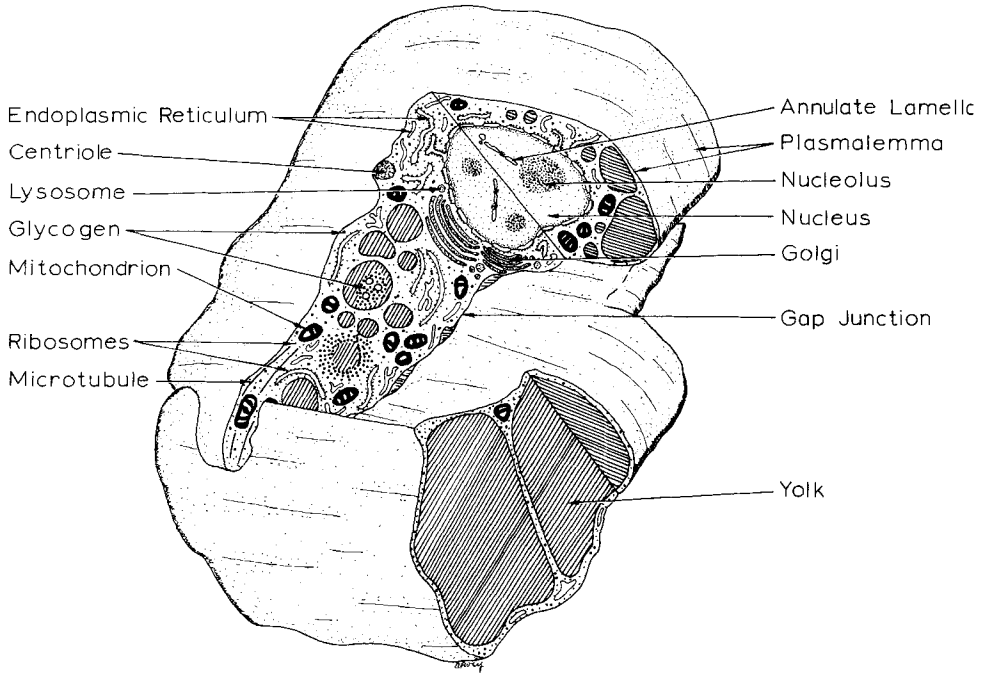


PLATE 3

EXPLANATION OF FIGURES

- 5 Schematic diagram of cells in the muscle bands of the vesiculate embryo (stage IV of caudal myogenesis). The illustrated cells are typical of those located in either the dorsal or the ventral part of the muscle band (table 2). The long axis of the cell is now parallel to the long axis of the muscle band (fig. 1).
- 6 Schematic diagram of cells in the muscle bands of the papillate embryo (stage V of caudal myogenesis). The depicted cells are representative of those situated in the dorsal and ventral parts of the muscle band (table 2). The long axis of the cell is parallel to the long axis of the muscle band (fig. 1). (The sarcoplasmic reticulum has been omitted from the drawing.)

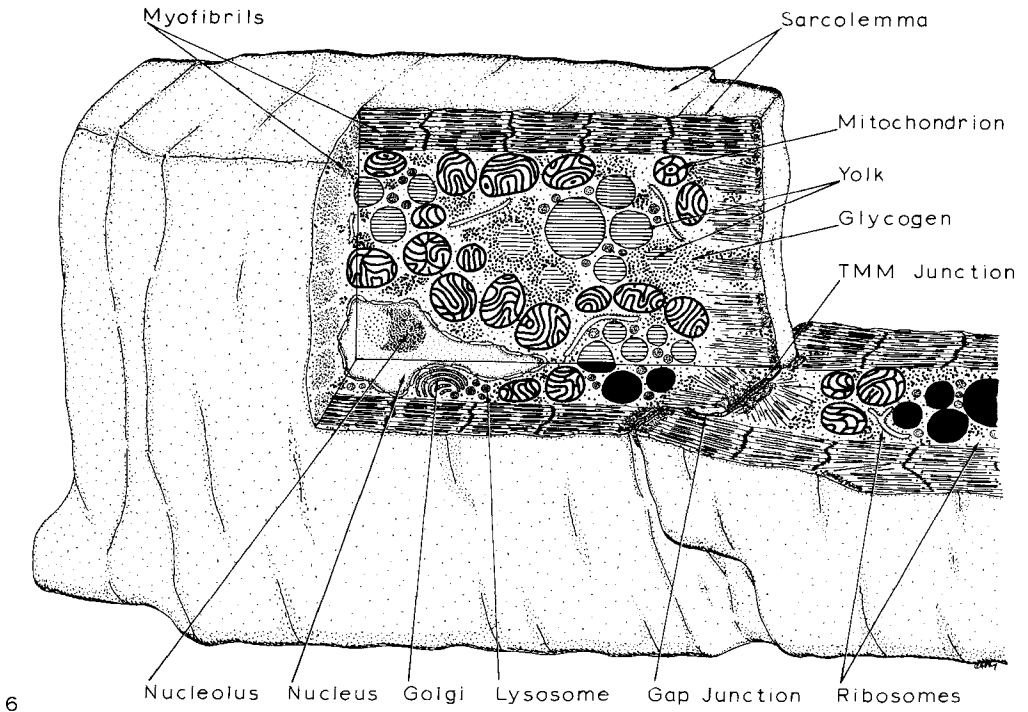
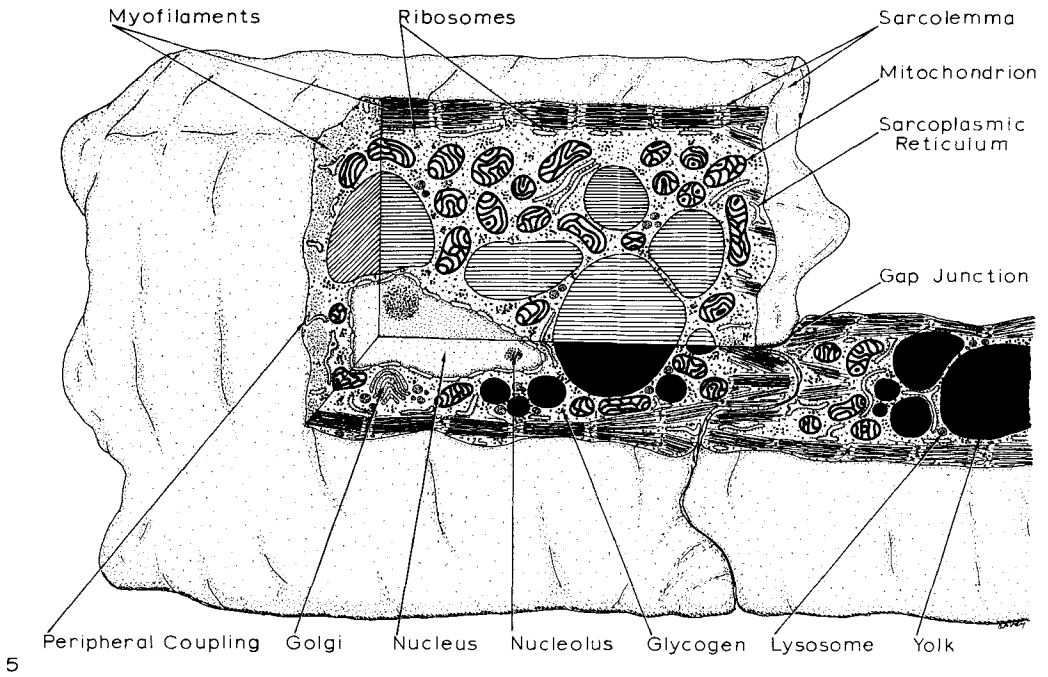


PLATE 4

EXPLANATION OF FIGURES

- 7 Schematic diagram of cells in the muscle bands of the prehatching tadpole (stage VI of caudal myogenesis). The illustrated cells would be found in either the dorsal or the ventral part of the muscle band (table 2). The long axis of the cell is parallel to the long axis of the muscle band (fig. 1). (The sarcoplasmic reticulum has been omitted from the drawing.)
- 8 Absolute cytoplasmic volume occupied by the classes of organelles in differentiating caudal muscle cells. Roman numerals designate the seven stages of caudal myogenesis used in this study (consult fig. 1). The collated data contained in table 4 are displayed as functions of the stage of differentiation. The data are plotted on the vertical lines, and points between successive vertical lines are extrapolations. The spacings between the vertical lines (stages of caudal myogenesis) are proportional to time (table 1).
- 9 Relative cytoplasmic volume occupied by the classes of organelles in differentiating caudal muscle cells. Roman numerals designate the seven stages of caudal myogenesis used in this study (consult fig. 1). The collated data contained in table 4 are displayed as functions of the stage of differentiation. The data are plotted on the vertical lines, and points between successive vertical lines are extrapolations. The spacings between the vertical lines (stages of caudal myogenesis) are proportional to time (table 1).

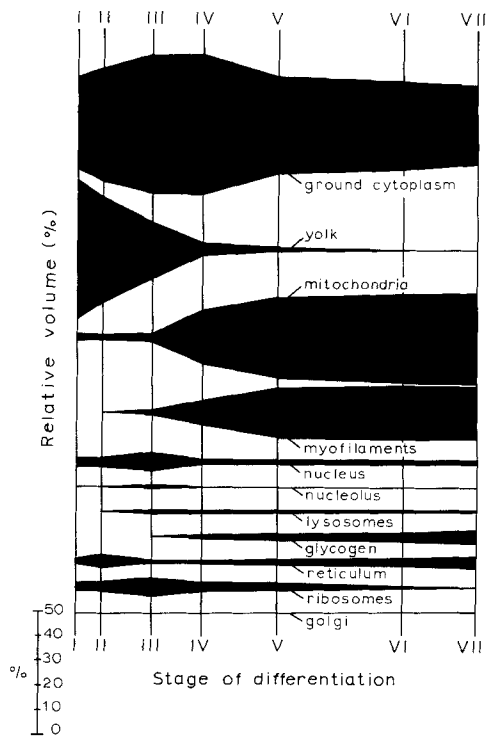
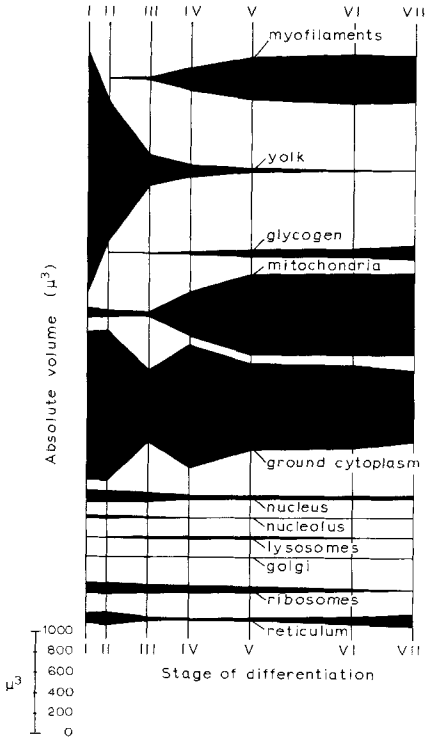
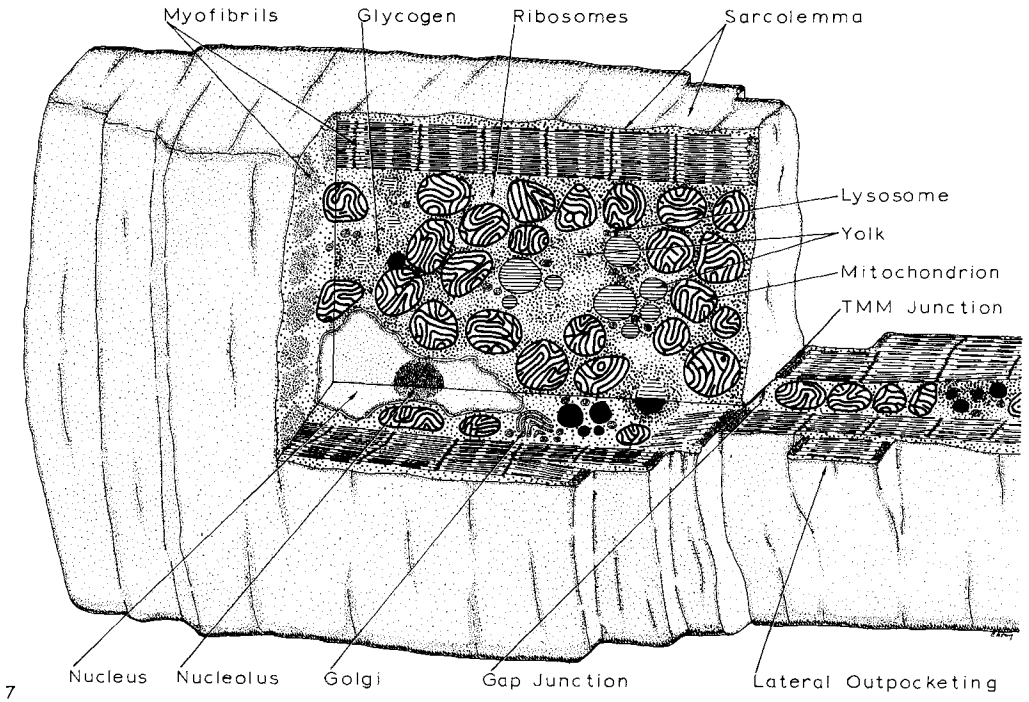


PLATE 5

EXPLANATION OF FIGURES

- 10 Photomicrograph (dorso-lateral view) of the neurulating embryo (I). Myoblasts are segregated into two bands beneath the epidermis in the caudal rudiment. Consult the text for a description of other anatomical features. Living specimen, $\times 50$. Calibration bar = 0.1 mm.
- 11 Longitudinal thin section through the nuclear regions of two adjacent myoblasts of the neurulating embryo (I). The single, ovoid nucleus within each cell contains large nucleoli and segments of annulate lamellae. The rough-surfaced endoplasmic reticulum derives from evaginations of the nuclear envelope (arrow) and accumulates in a perinuclear zone. Proteid-yolk granules occupy most of the cytoplasmic volume and displace the nucleus to the peripheral cytoplasm, a short distance from the plasmalemma. Mitochondria with simple cristae are prevalent in the region of the nucleus. The ground cytoplasm contains darkly staining ribosomes and discrete glycogen granules of low electron density. Cacodylate-buffered glutaraldehyde/bicarbonate-buffered osmium fixation, $\times 22,800$.
- 12 Photomicrograph (lateral view) of the caudate embryo (II). Myoblasts in the caudal bud are actively dividing, and the length of the two presumptive muscle bands is less than one-third the circumference of the trunk. Consult the text for a description of other anatomical features. Living specimen, $\times 50$. Calibration bar = 0.1 mm.
- 13 Longitudinal thin section through the nuclear regions of two adjacent myoblasts of the caudate embryo (II). Most of the cellular volume is occupied by proteid-yolk granules which displace the ovoid nucleus peripherally until it is proximal to the plasmalemma. Evaginations of the nuclear envelope (arrow) produce rough-surfaced endoplasmic reticulum. Small mitochondria and multiple Golgi bodies reside near the nucleus. Electron dense ribosomes and electron lucent glycogen granules cohabit the ground cytoplasm. Cacodylate-buffered glutaraldehyde/bicarbonate-buffered osmium fixation, $\times 22,800$.

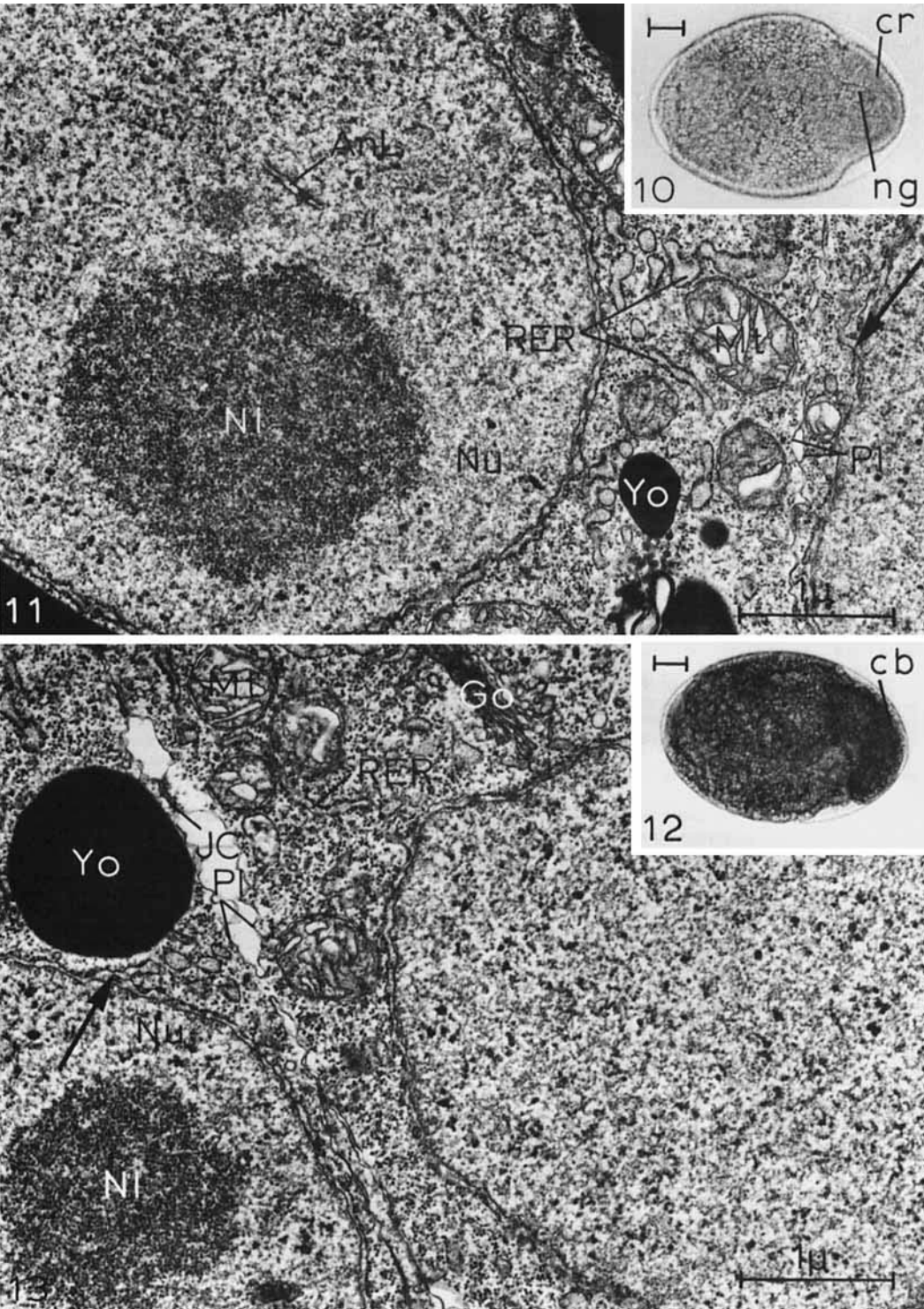


PLATE 6

EXPLANATION OF FIGURES

- 14 Photomicrograph (lateral view) of the comma embryo (III). The length of the elongating tail measures one-third to one-half the circumference of the trunk. The caudal tissues lie in a shallow, ventral groove of the trunk. Consult the text for a description of other anatomical features. Living specimen, $\times 50$. Calibration bar = 0.1 mm.
- 15 Longitudinal thin section through the sarcoplasm subadjacent to the nuclei of caudal muscle cells of the comma embryo (III). Note the variation in sarcoplasmic density, resulting from the relative concentrations of ribosomes and glycogen granules, between adjacent cells. Rough-surfaced sarcoplasmic reticulum and smooth-surfaced sarcoplasmic reticulum are visible in the cells. Individual myofilaments and networks of myofilaments (arrow) are usually restricted to the peripheral sarcoplasm but occasionally occur deep in the endoplasm. Mitochondria are small in diameter and have simple cristae. The envelope of the nucleus is perforated, and polysomes are associated with the pores. Junctional complexes between sarcolemmata are scarce. Intracellularly, short segments of smooth-surfaced SR closely approach the sarcolemma. Cacodylate-buffered glutaraldehyde/bicarbonate-buffered osmium fixation, $\times 29,100$.
- 16 Transverse thin section through the overlapping thick and thin myofilaments in a network in a caudal muscle cell of the comma embryo (III). Bridges (arrows) between the thick and thin myofilaments are indicated, and the thick myofilaments are observed to have an incomplete complement of thin myofilaments. Bicarbonate-buffered osmium fixation, $\times 127,700$.
- 17 Transverse thin section through the thick myofilaments in a network in a caudal muscle cell of the comma embryo (III). H-bridges (arrows) interconnect the naked central shafts of the thick myofilaments. Bicarbonate-buffered osmium fixation, $\times 127,700$.
- 18 Transverse thin section of a differentiating peripheral coupling in a caudal muscle cell of the comma embryo (III). The subsarcolemmal cisterna of SR and the sarcolemma are in close apposition. Segments of the subsarcolemmal cisterna distant from the cellular membrane continue to bind ribosomes. Cacodylate-buffered glutaraldehyde/bicarbonate-buffered osmium fixation, $\times 48,900$.

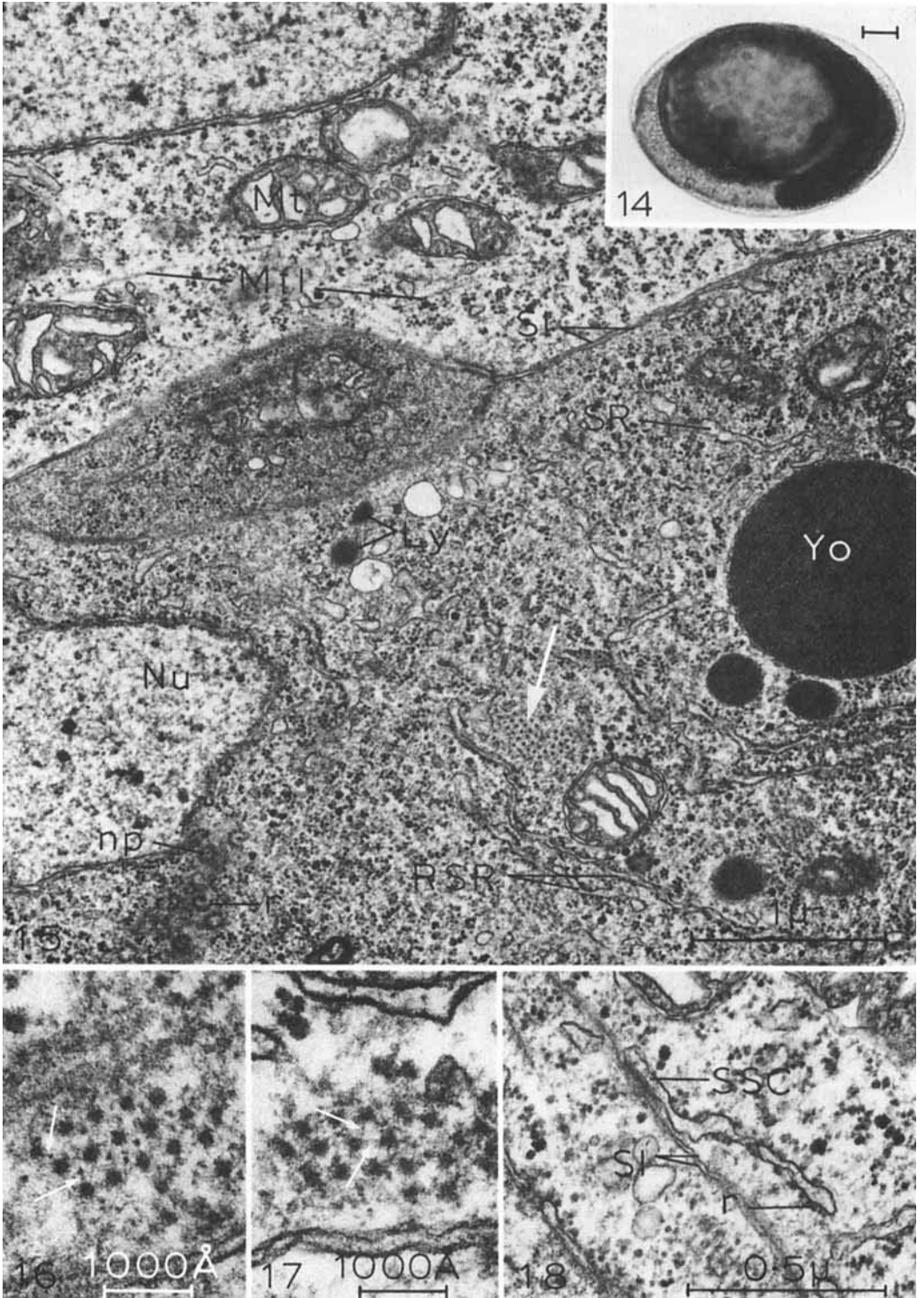


PLATE 7

EXPLANATION OF FIGURES

- 19 Photomicrograph (lateral view) of the vesiculate embryo (IV). The two caudal muscle bands, flanking the notochord, measure about two-thirds of their final length and are undergoing a 90° rotation along with the other caudal tissues. Consult the text for a description of other anatomical features. Living specimen, × 40. Calibration bar = 0.1 mm.
- 20 Longitudinal thin section of the caudal muscle cells of the vesiculate embryo (IV). The envelope of the elongate nucleus is perforated, and polysomes are associated with the pores. Myofilaments (large arrow) are apposed to the peripheries of the nascent myofibrils. The abundant rough-surfaced sarcoplasmic reticulum is continuous (small arrow) with the smooth-surfaced sarcoplasmic reticulum which forms peripheral couplings with the sarcolemma. Ribosomes, associated with the nuclear envelope and bound to the reticular membranes, also reside in the sarcoplasm and are interspersed with glycogen granules. Close junctions between sarcolemmata are increasing in frequency. Cacodylate-buffered glutaraldehyde/bicarbonate-buffered osmium fixation, × 27,900.
- 21 Longitudinal thin section of the transverse boundaries of the caudal muscle cells of the vesiculate embryo (IV). Each muscle cell has a cortical row of nascent myofibrils, but the sarcolemmata do not form transverse myomuscular junctions and are only engaged in the formation of close junctions. Thin myofilaments from the terminal sarcomeres closely approach and even contact the sarcolemma at the transverse cellular boundary. Cacodylate-buffered glutaraldehyde/bicarbonate-buffered osmium fixation, × 28,500.
- 22 Longitudinal thin section of the lateral boundaries of the caudal muscle cells of the vesiculate embryo (IV). Apposed sarcolemmata participate in the formation of close junctions and peripheral couplings with cisternae of the sarcoplasmic reticulum in the field of myofilaments. The gap of the peripheral coupling is occupied by a dense plaque (arrow) lying equidistant from the two apposed membranes. Cacodylate-buffered glutaraldehyde/bicarbonate-buffered osmium fixation, × 47,400.

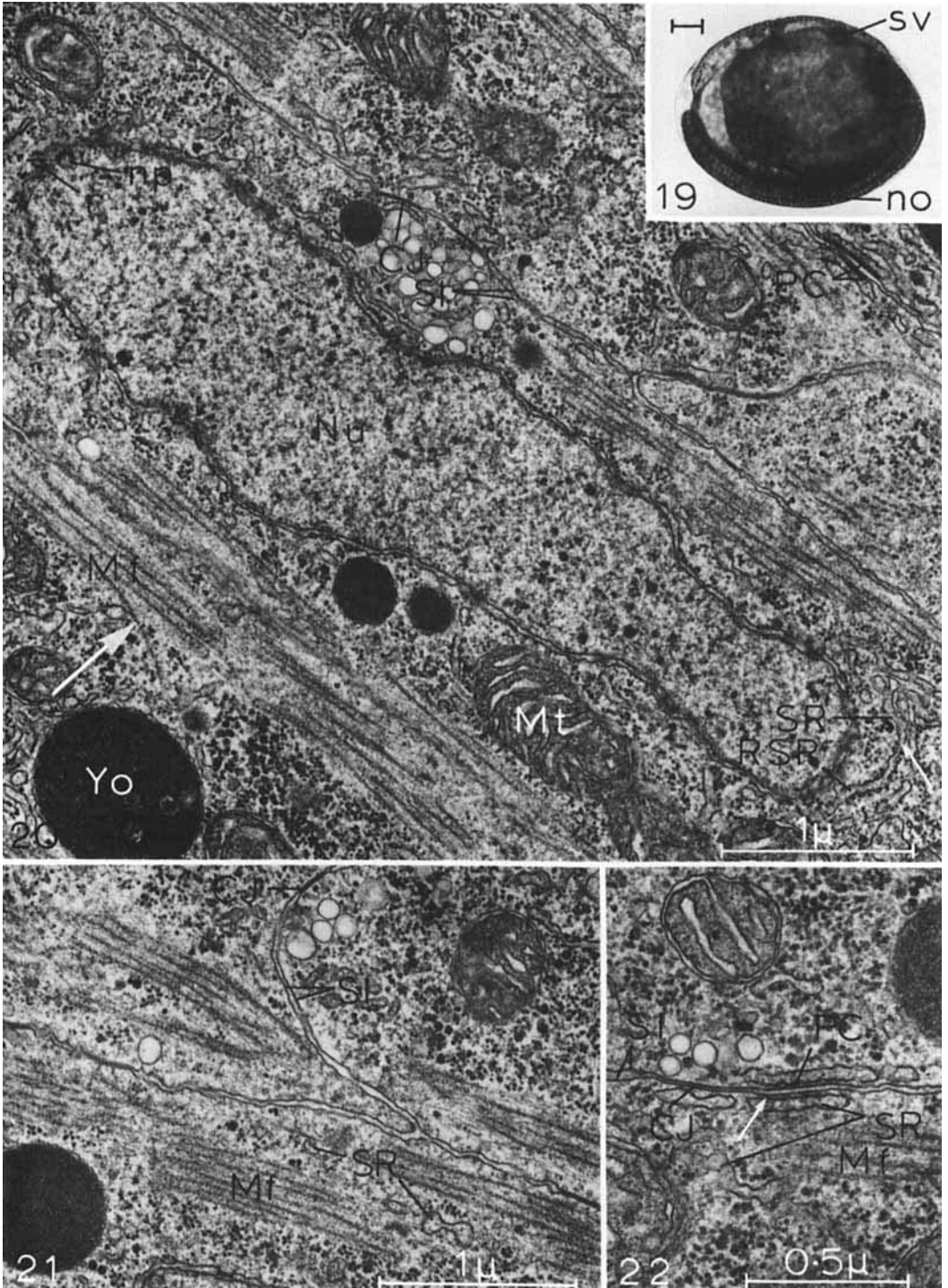


PLATE 8

EXPLANATION OF FIGURES

- 23 Photomicrograph (lateral view) of the papillate embryo (V). The two caudal muscle bands are nearly full length. Consult the text for a description of other anatomical features. Living specimen, $\times 35$. Calibration bar = 0.1 mm.
- 24 Longitudinal thin section of the caudal muscle cells of the papillate embryo (V). The epidermis with associated basal lamina is visible at the top of the micrograph. The muscle band is surrounded by a thin external lamina. Portions of two muscle cells are shown, however the boundary between them (arrows) is not distinct because the section grazes the sarcolemmata. Z-lines, I-bands, and A-bands are evident in the peripherally located myofibrils. The sarcoplasmic reticulum investing the myofibrils is smooth-surfaced, and segments of rough-surfaced SR frequently occur in the endoplasm. A central nucleus, numerous mitochondria, small proteid-yolk granules, and putative primary lysosomal granules also reside in the endoplasm. Cacodylate-buffered glutaraldehyde/bicarbonate-buffered osmium fixation, $\times 29,600$.
- 25 Longitudinal thin section of a differentiating myomuscular junction between the caudal muscle cells of the papillate embryo (V). Myofibrils insert at the myomuscular junction at a sarcomeric level corresponding to a Z-line. Thin myofilaments of the terminal halves of the I-bands are obscured by amorphous material, or Z-matrix. A dense layer of material is situated equidistant from the two apposed sarcolemmata in the extracellular space of the junction. Cacodylate-buffered glutaraldehyde/bicarbonate-buffered osmium fixation, $\times 43,900$.
- 26 Longitudinal thin section of the extracellular space of a differentiating myomuscular junction between the caudal muscle cells of the papillate embryo (V). The apposed sarcolemmata are separated by an extracellular space approximately 350 Å wide. Extracellular thin filaments (arrows) traverse the junctional space at right angles to the sarcolemmata, penetrating the central dense layer. Cacodylate-buffered glutaraldehyde/bicarbonate-buffered osmium fixation, $\times 60,600$.

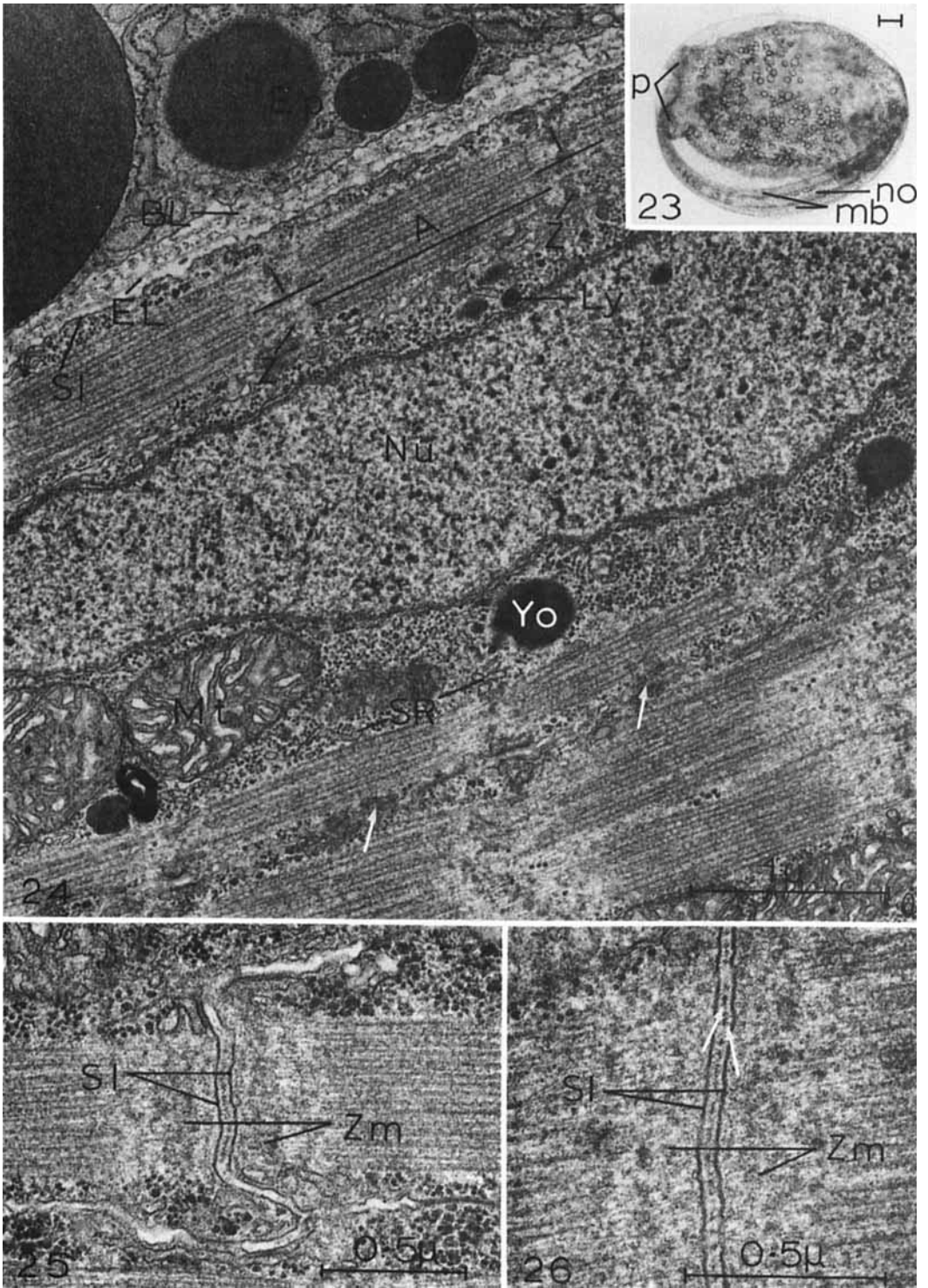


PLATE 9

EXPLANATION OF FIGURES

- 27 Transverse thin section of the caudal muscle cells of the papillate embryo (V). The cortical row of myofibrils in each sectioned cell is cut through various sarcomeric levels. The endoplasm contains very short segments of rough-surfaced sarcoplasmic reticulum, and the smooth-surfaced SR invests the myofibrils and establishes peripheral couplings with the sarcolemma. Close junctions between the sarcolemmata are prevalent. Cacodylate-buffered glutaraldehyde/bicarbonate-buffered osmium fixation, $\times 23,900$.
- 28 Transverse thin section through the I-bands of myofibrils in the caudal muscle cells of the papillate embryo (V). Myofibrils are cut through the Z-lines, I-bands, and A-bands. The transverse collar of sarcoplasmic reticulum centered on the Z-line forms peripheral couplings with the sarcolemma and invests the myofibril as a single, perforated sheet. Cacodylate-buffered glutaraldehyde/bicarbonate-buffered osmium fixation, $\times 33,100$.
- 29 Transverse thin section through the H-bands of myofibrils in the caudal muscle cells of the papillate embryo (V). Myofibrils are cut through the I-bands, A-bands, and H-bands. A collar of sarcoplasmic reticulum embracing the H-band incompletely invests the myofibril as a single layer. Cacodylate-buffered glutaraldehyde/bicarbonate-buffered osmium fixation, $\times 33,100$.

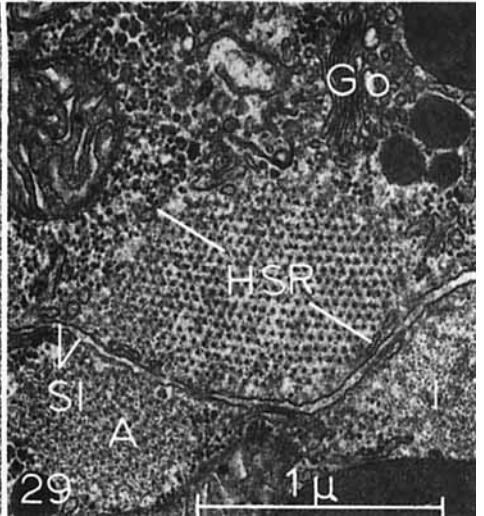
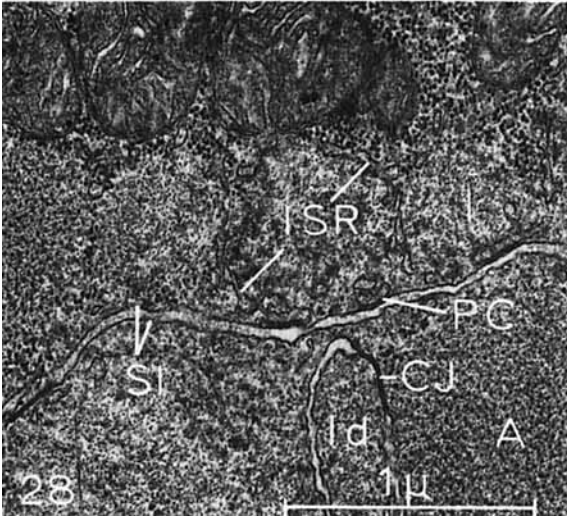
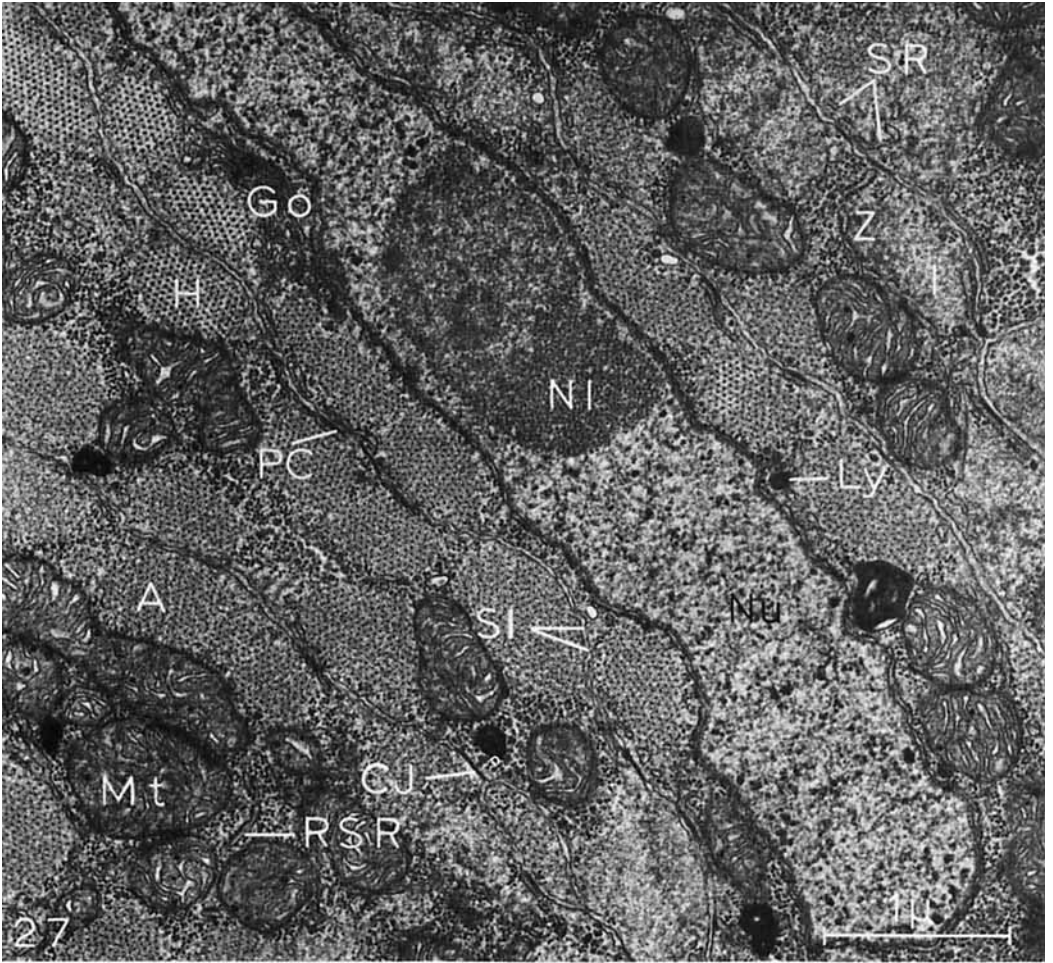


PLATE 10

EXPLANATION OF FIGURES

- 30 Photomicrograph (lateral view) of the prehatching tadpole (VI). The two caudal muscle bands have nearly reached their full length and are contracting sporadically. Consult the text for a description of other anatomical features. Living specimen, $\times 35$. Calibration bar = 0.1 mm.
- 31 Longitudinal thin section of the caudal muscle cells of the prehatching tadpole (VI). The cortical row of myofibrils is characterized by slightly irregular I-bands and obscured Z-lines. A-bands have distinct H-bands with central M-lines. Myofibrils are invested with sarcoplasmic reticulum, and cisternae of SR form peripheral couplings with the sarcolemma. Mitochondria with an elaborate serpentine pattern of cristae underlie the myofibrils, and an elongate nucleus is centrally situated within each cell. Only small proteid-yolk granules remain in the endoplasm, and numerous putative primary lysosomal granules are present. Close junctions between apposed sarcolemmata are quite numerous. Cacodylate-buffered glutaraldehyde/bicarbonate-buffered osmium fixation, $\times 22,800$.
- 32 Longitudinal thin section of a transversely oriented myomuscular junction between the caudal muscle cells of the prehatching tadpole (VI). Amorphous material associated with the thin myofilaments in the terminal halves of the I-bands accumulates into zones of Z-matrix, separated from the sarcolemma by an area of low electron density. Cacodylate-buffered glutaraldehyde/bicarbonate-buffered osmium fixation, $\times 43,900$.
- 33 Longitudinal thin section of an obliquely oriented myomuscular junction between the caudal muscle cells of the prehatching tadpole (VI). Most of the myomuscular junctions between cells are orthogonally oriented with respect to the primary axes of the myofibrils, but a few obliquely oriented junctions persist. Cacodylate-buffered glutaraldehyde/bicarbonate-buffered osmium fixation, $\times 43,900$.
- 34 Longitudinal thin section of the extracellular space of a myomuscular junction between the caudal muscle cells of the prehatching tadpole (VI). The apposed sarcolemmata are separated by an extracellular space that is approximately 550 Å wide. Extracellular thin filaments (arrows) traverse the space at right angles to the sarcolemmata. An area of low electron density is interposed between the sarcolemma and the Z-matrix. Cacodylate-buffered glutaraldehyde/bicarbonate-buffered osmium fixation, $\times 60,600$.
- 35 Longitudinal thin section of a junctional complex between the plasmalemmata of myoblasts of the caudate embryo (II). Apposed plasmalemmata are separated by an extracellular space that is approximately 250 Å wide. Electron dense material in the extracellular space occasionally accumulates into two layers. Cacodylate-buffered glutaraldehyde/bicarbonate-buffered osmium fixation, $\times 104,900$.
- 36 Longitudinal thin section of a close junction between the sarcolemmata of caudal muscle cells of the prehatching tadpole (VI). The extracellular gap of the fully differentiated close junction is 30–40 Å wide. Cacodylate-buffered glutaraldehyde/bicarbonate-buffered osmium fixation, $\times 104,900$.
- 37 Longitudinal thin section of a differentiating close junction between the sarcolemmata of caudal muscle cells of the prehatching tadpole (VI). The sarcolemmata assume a constant separation of 350 Å, and the extracellular thin filaments (arrows) penetrate a fibrous layer situated equidistant from the two sarcolemmata. Cacodylate-buffered glutaraldehyde/bicarbonate-buffered osmium fixation, $\times 104,900$.

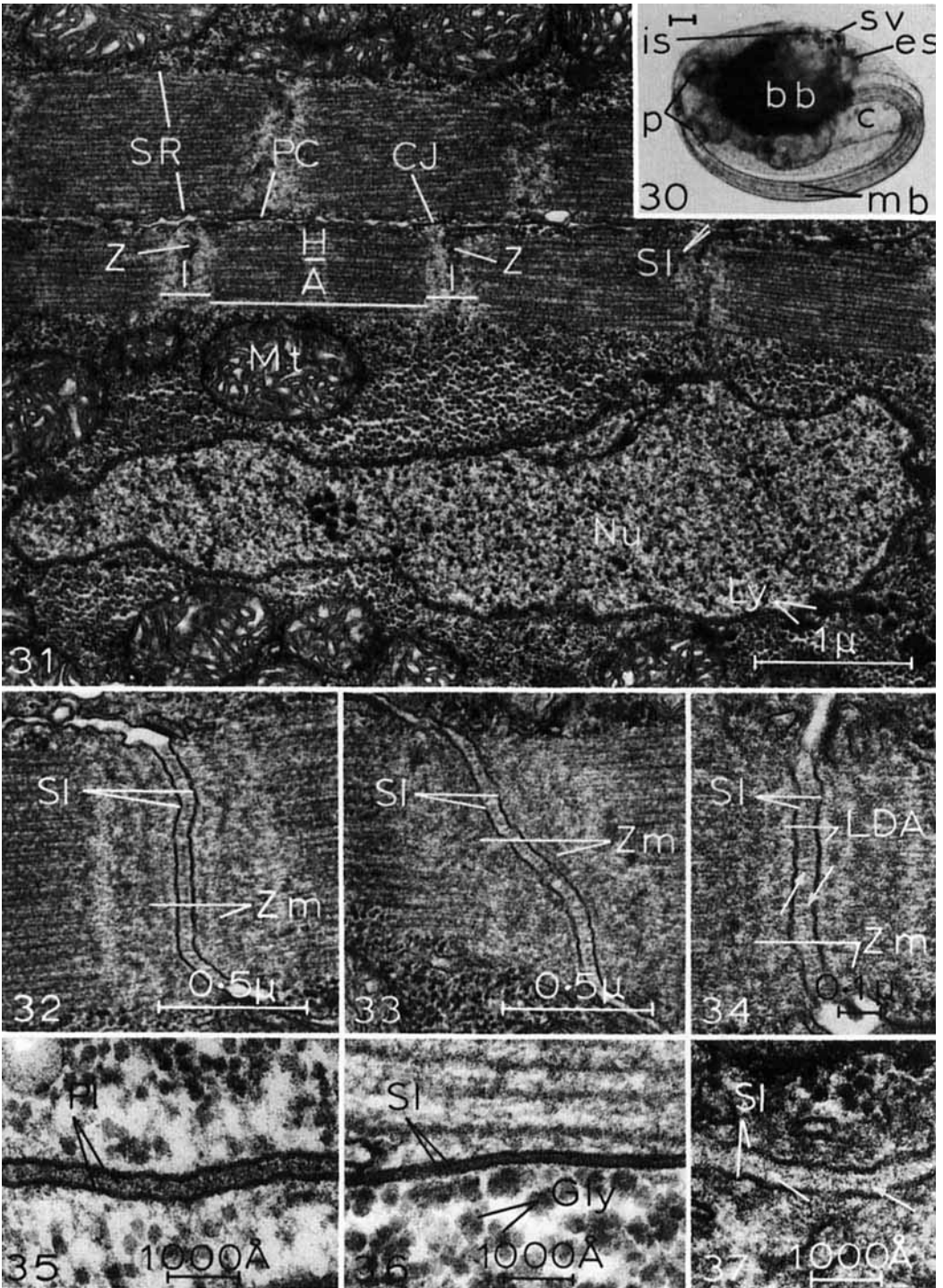


PLATE 11

EXPLANATION OF FIGURES

- 38 Transverse thin section of the caudal muscle cells of the prehatching tadpole (VI). Portions of three muscle cells are shown. The sarcolemmata participate in the formation of both close junctions and peripheral couplings with subsarcolemmal cisternae of the sarcoplasmic reticulum. A collar of SR is centered on the sarcomeric Z-line and embraces the I-band. A second collar of SR, centered on the M-line and extending laterally to the boundaries with the A-bands, invests the H-band as one complete layer. The sheet is discontinuous (arrows) at the side of the myofibril most distant from the cellular membrane, and the ends of the sheet are frequently observed to elevate from the surface of the myofibril. Multilamellar bodies in the sarcoplasm are probably indicative of lysosomal activity. The ground sarcoplasm contains numerous mitochondria and is rich in glycogen granules. Cacodylate-buffered glutaraldehyde/bicarbonate-buffered osmium fixation, $\times 31,900$.
- 39 Longitudinal thin section of the lateral boundaries of caudal muscle cells of the prehatching tadpole (VI). Sarcolemmata are intimately apposed at close junctions. Regions of the sarcolemmata that will probably form close junctions possess a fibrous material in the intervening extracellular space (large arrow). Peripheral couplings are interspersed between the close junctions and are commonly localized near the sarcomeric Z-lines. A dense plaque (small arrow) lies in the gap of the peripheral coupling, equidistant from the two apposed membranes. Cacodylate-buffered glutaraldehyde/bicarbonate-buffered osmium fixation, $\times 39,200$.

